NASA Contractor Report 3008

A Comparison of Wake Characteristics of Model and Prototype Buildings in Transverse Winds

Earl Logan, Jr., Prapoj Phataraphruk,
and Jingfa Chang

CONTRACT NAS8-32357
MAY 1978

NASA

NASA Contractor Report 3008

A Comparison of Wake Characteristics of Model and Prototype Buildings in Transverse Winds

Earl Logan, Jr., Prapoj Phataraphruk,
and Jingfa Chang
Arizona State University
Tempe, Arizona

Prepared for
George C. Marshall Space Flight Center
under Contract NAS8-32357

NASA
National Aeronautics
and Space Administration

**Scientific and Technical
Information Office**

1978

FOREWORD

This study was initiated to determine the feasibility of predicting wake profiles behind buildings and natural obstacles using a scaled model in a wind tunnel. The wind tunnel approach is preferable because of economy of time and money, simplicity and convenience. This is the first report of a continuing program sponsored by the Fluid Dynamics Branch, Atmospheric Sciences Division of the Space Sciences Laboratory at the George C. Marshall Space Flight Center, National Aeronautics and Space Administration, Huntsville, Alabama.

This research was conducted under the technical direction of Mr. Dennis W. Camp and Mrs. Margaret Alexander of the Space Sciences Laboratory at Marshall Space Flight Center. The support for this research was provided by Mr. John Enders of the Aeronautical Operating Systems Division, Office of Advanced Research and Technology, NASA Headquarters.

TABLE OF CONTENTS

LIST OF TABLES

LIST OF FIGURES

NOMENCLATURE

f	Coriolis parameter
H	height of building or model
k	von Karman constant
K	constant in Counihan-Hunt-Jackson Theory calculated from Eq. 13
M	subscript for model
MOM	Momentum flow per unit width
n	power law exponent
P	subscript for prototype
T1,T2,T3,T4,T5,T6	meteorological towers Nos. 1,2,3,4,5,6
U	horizontal component of air velocity of any z
U_H	horizontal component of air velocity at z = H upstream of building
U_M	horizontal component of air velocity at $z = \delta_L$ upstream of model
U_r	horizontal component of air velocity far upstream of building (T1) at z/H = 6.5
U_∞	geostrophic or free stream wind velocity
ΔU	velocity deficit based on upstream velocity
u^*	friction velocity, $(\tau_o/\rho)^{1/2}$
u'	RMS of fluctuation of horizontal component of air velocity at any z
z	elevation
z_o	roughness length
δ	model or prototype boundary layer thickness
δ_L	height of surface layer, i.e., logarithmic layer
ζ	dimensionless velocity deficit defined by Eq. 12

η	dimensionless height z defined by Eq. 11
θ	wind direction, θ = 180° for wind from T1 to T6 (wind from N 30° W)
λ	geographic latitude
ν	kinematic viscosity of the air
ρ	density of air
τ	shear stress τ_{zx}
τ_o	surface shear stress
ω	earth's rotation rate

CHAPTER 1

INTRODUCTION

The work described in this report is motivated by the need to understand the wind environment around air terminals. Ascent or descent of aircraft through the atmospheric boundary layer is accompanied by changes in lift associated with changes in wind speed with altitude. The acceleration produced by the brief action of unbalanced forces results in deviations from the original flight path for descending flight. The above effect is enhanced by induced flows produced by buildings or natural obstacles in the vicinity of airports. The effect of these surface obstacles on the aerospace environment around airports has been reviewed recently by Fichtl, et al. [1]. Shear layers, or wakes, produced downwind of surface obstacles can prove hazardous to aircraft, especially those of the V/STOL type, because of the high rate of change of wind speed with altitude in the layer. Clearly research is needed to determine the locations of these regions of induced flows in the wakes of surface obstacles and their effects on aeronautical systems.

Related theoretical and experimental research has been carried out in recent years. Most of the pertinent literature has been discussed in extensive literature surveys by Fichtl, et al. [1] and by Frost [2]. Some of the work cited in these references appear to be useful in the present study.

A particularly useful theoretical study has been reported by Counihan, et al. [3]. A theoretical framework is provided for correlating experimental wake measurements corresponding to a given building geometry and upstream profile characteristics. Models of long buildings immersed in

a boundary layer having a thickness of ten times the model height have been used by Woo, et al [4] to obtain measurements of wake velocity and turbulence. The data of Woo, et al [4] are expected to be useful in testing the predictions based on the theory of Counihan, et al [3].

Other experimental studies are also helpful in giving insight into the physics of the wake flow. Oka and Kostic [5] made detailed measurements of velocity and turbulence in the recirculation region behind a two-dimensional square rod placed on one wall of a channel of rectangular cross section. Mueller and Robertson [6] measured wake profiles behind two-dimensional obstacles of quarter-round cross section including both data in the recirculation region and far downstream. Good and Joubert [7] studied the aerodynamic drag of bluff plates and obtained useful correlations between upstream conditions and plate height. These relations should be useful in predicting the effect of obstacle height on wake profiles.

Most of the available reports of experimental research dealing with wake flow behind obstacles are based on work done with small scale laboratory equipment. Few field studies have been made, however, major studies have been reported by Frost and Shahabi [8], Frost, et. al [9] and Sacre [10]. In the work of Frost and Shahabi the wake of a simulated block building was studied under field conditions using ten instrumented wind towers located at Marshall Space Flight Center's Atmospheric Boundary Layer Facility (ABLF). The anemometers and vanes supported on the towers were used to measure mean horizontal wind profiles, wind direction and vertical wind speed. In addition to the three components of wind, the turbulence components were also measured. The tower locations are shown schematically in Fig. 1, where T1, T2, T3,

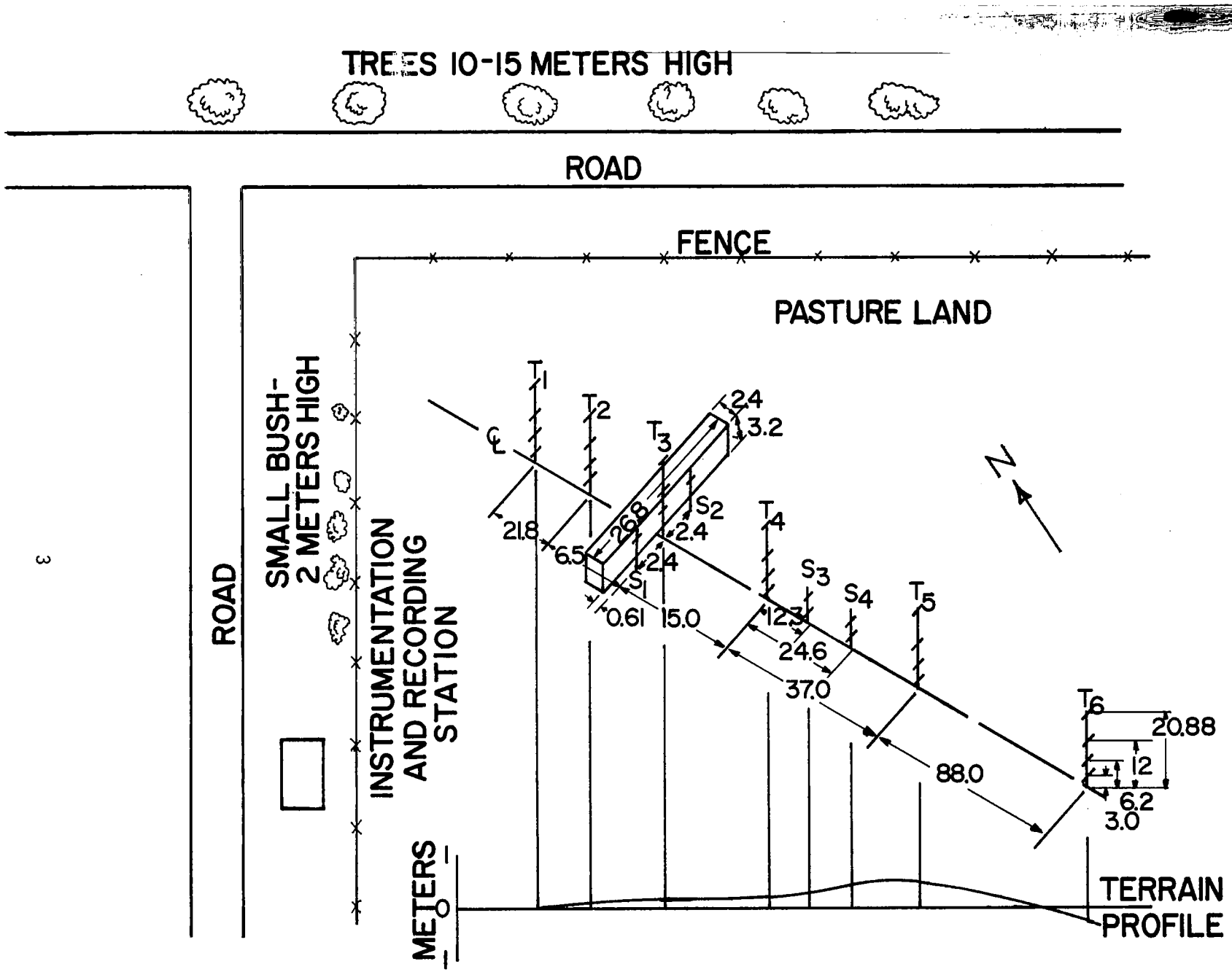

Fig. 1 MSFC Atmospheric Boundary Layer Facility

T4, T5, and T6 are used to denoted the six principal towers used in the investigation. The distances given in Fig. 1 are in meters, and the dimensions of the simulated block building are indicated as height 3.2m, width 2.4m and length 26.8m. The investigation considered primarily winds in the direction from T1 to T6, i.e., winds from North 30° West. The last measuring station (T6) is located about 44 building heights downwind of the simulated building, i.e., x/H = 44 at tower T6. The instruments were located on the towers at 3, 6.2, 12 and 20.88m above the ground, i.e., at z/H equal to 0.94, 1.94, 3.75 and 6.5, respectively. Thus wind profiles up to 6.5 building heights above the ground are measured at several stations starting eight building heights upwind of the building (T1) and extending to 44 building heights downwind of the building (T6). The boundaries of this wake study clearly encompass the principal regions of affected wind present in the flow. Too, these wind profiles are contained in the region traversed in the wind tunnel investigation of Woo, et al [4].

The wind tunnel investigation of Woo, et al [4] was carried out in the Meteorological Wind Tunnel (MWT) in the Fluid Dynamics and Diffusion Laboratory at Colorado State University (CSU) using several models of buildings, one of which was a 1/50-scale model of the 3.2 x 2.4 x 26.8m building depicted in Fig. 1 and used in the field study at MSFC-ABLF. The upstream profile was simulated by using the appropriate artificial roughness on the wall of the wind tunnel. Both mean and fluctuating velocities were measured in the wake of the model building. Profiles were measured at several downstream stations in the wake including four which correspond exactly to the locations of towers T4, S3, S4, and T5. Thus it is possible to use the wind tunnel data to compare with the actual field data taken in the atmospheric boundary layer.

The present work is a preliminary comparison of the MSFC-ABLF field data and the CSU-MWT wind tunnel data. The purpose of the comparison is to assess the accuracy of predicted wake profiles for the prototype building based on measurements made in the wake of the wind tunnel model, and to arrive at conclusions as to how disparities can be reduced or eliminated. Accurate prediction of building wakes for the purpose of mapping the wind environment of aircraft near terminals is most economically accomplished by wind tunnel modeling. However, evidence that wind tunnel wake data can be correlated with full-scale wake results is a necessary step in the establishment of the reliability of the technique.

CHAPTER 2

COMPARISON OF UPSTREAM CONDITIONS

This chapter is devoted to the characteristics of velocity profiles upstream of the building or model. Referring to Fig. 1 for the field tower arrangement, the upstream profile is that measured at the first tower, Tower T1, assuming a wind direction from T1 to T6, i.e., the wind angle* θ is 180°. The profile so determined can be characterized by the exponent n found in the power law

$$\frac{U}{U_\infty} = \left(\frac{z}{\delta}\right)^n \tag{1}$$

This relation models the entire boundary layer, and the exponent n can be determined from velocity profiles measured either in the field or in the wind tunnel without knowing U_∞ or δ. The exponent n is the slope of the straight line graph which represents U versus z on log-log paper. The surface or logarithmic layer has a velocity distribution which fits

$$\frac{U}{u^*} = \frac{1}{k} \ln \frac{z}{z_o} \tag{2}$$

where u* and z_o are the velocity and length scales, respectively, for this layer. The friction velocity u* can also be determined from the velocity profile measured in the wind tunnel or the field without knowing the roughness length. The friction velocity is simply obtained from the slope of the plot of U versus ln z.

---

*where θ is defined to be the direction of alignment of the towers and is not measured from north. The towers are aligned approximately 30° off (west) from north.

Table 1 consists of values of friction velocity for five tower locations and of upstream power law exponent determined by the least squares method. The results of these calculations for runs having a wind direction θ of approximately 180°, i.e., north 30° west, are presented in Table 1. Some values are omitted because of nonlinearity or insufficiency of data. The origin of the x-coordinate is at the downwind face of the building; thus the towers T1 and T2 are located at x/H values of -8.65 and -1.84, respectively, and T4, T5 and T6 have x/H values of 4.88, 16.44 and 43.94, respectively. Runs 8013-8038 were made without a building, and Runs 8407-8512 were made with the building in place.

The upstream wind profile exponent observed in the field is clearly affected by the presence of the trees and bushes shown in Fig. 1 upwind of the first tower. Since tests were carried out over a period of three years and the size of the natural vegetation changed during this time, it is to be expected that the exponent n would change. The 1972 values were 0.14-0.19, while the 1974 values varied from 0.24-0.31. Additionally, T1 was located 3.5m* (x/H = -2.93) from T2 in 1972 as compared with the 21.8m distance used in 1974 as shown in Fig. 1. Deviation of wind direction from 180° also produced variation of the exponent. The values of u* depend on the upstream surface roughness, the size of obstacles and the geostrophic wind velocity U_∞. Thus considerable variation of u* is observed at Tower T1.

A variety of related model testing was done in the CSU-MWT and is reported by Woo, et al [4]. The test condition and model

---

*This distance applies to Runs 8013-8038 in Table 1.

Table 1. Friction Velocity (m/s) for a Wind Direction of 180 Degrees

Run No.	Exponent n at T1	T1	T2	T4	T5	T6
8013	0.14	0.210	0.323	0.268	0.283	0.198
8018	0.14	0.252	0.302	0.448	0.299	0.269
8019	0.19	0.238	0.298	0.457	0.251	0.222
8038	--	--	--	0.242	0.328	0.225
8407	0.26	0.428	0.558	0.583	0.249	0.222
8408	0.25	0.388	0.559	0.566	0.413	0.223
8501	0.24	0.510	0.795	0.382	0.256	0.407
8502	0.28	0.635	0.828	0.762	0.530	0.431
8503	0.31	0.723	0.915	0.784	0.584	0.485
8504	0.26	0.552	0.808	0.809	0.474	0.423
8512	0.31	0.575	0.512	0.604	0.428	0.368

sizes used are presented in brief form in Table 2. The model tests of principal interest in the present comparison study are those for test condition No. 2 for which n = 0.27, δ = 0.61m, z_o = 0.0061m and U_∞ = 16m/s. A field run with an exponent close to this value is Run No. 8407 with n = 0.26 and u* = 0.428m/s. Equation (2) can be used to determine z_o for this field run. The resulting apparent roughness length is 0.16m, which is excessive. Profile data for other runs at T1 also yield excessive values; e.g., the calculated values of z_o are 0.226m, 0.254m and 0.591m for Run Nos. 8408, 8504 and 8512, respectively. This is an order of magnitude larger than the value determined by Frost, et al. [9], viz., z_o = 0.007m. The explanation for this follows from Equation (2) in the form

$$z_o = \frac{z}{\exp \frac{kU}{u^*}} \tag{3}$$

coupled with the observation that an obstacle causes an initial increase followed by a decay of u*, as can be observed from values given in Table 1 of this paper. Since the obstacles, i.e., trees, bushes, fences and ditches, upstream of Tower T1 initially raise the value of u*, and since u* decays very slowly, u* at Tower T1 is expected to be larger than its equilibrium value, and Equation (3) shows that the corresponding calculated value of z_o should also be higher. On the other hand, Equation (3) yields values of z_o of 0.0107m and 0.0116m at Tower 6 for Run Nos. 8504 and 8512, respectively, which are reasonable values of roughness length for the terrain used.

It is clear that care must be exercised in modeling atmospheric flows by simply adjusting wind tunnel power law exponents. Although the velocity profiles for wind tunnel condition No. 2 and field Run No. 8407 have

Table 2. Geometric Condition for Modeling in CSU-MWT

Test Condition	δ(m)	z_o(mm)	δ/z_o	Model 1		Model 2		Model 3		Model 4	
				H/δ	H/z_o	H/δ	H/z_o	H/δ	H/z_o	H/δ	H/z_o
1	0.71	4.3	165	0.044	7.21	0.0915	15.1	0.116	19.2	0.090	14.9
2	0.61	6.1	100	0.051	5.08	0.1066	10.7	0.135	3.5	0.105	10.5
3	0.38	0.11	3455	0.082	281.8	0.171	591	0.217	751	0.168	582
4	1.37	0.048	28542	0.023	645.8	0.047	1354	0.060	1721	0.047	1333

approximately the same characteristic exponent, i.e., $n \simeq 0.27$, the upstream wind tunnel profile is an equilibrium profile deriving from the uniform surface roughness of the wind tunnel wall, but the field profile at Tower T1 is a non-equilibrium profile in which turbulence generated by upstream obstacles is still decaying in the flow direction. Thus there is reason to expect some dissimilarity in the wake profiles of the model and prototype at stations downstream of the building resulting from differences in upstream velocity profiles. Dissimilarity of model and prototype wake flow fields would also be expected if geometric or turbulence dissimilarities were present in the upstream flow.

CHAPTER 3

CONDITIONS OF SIMILARITY

Cermak [11] and Sundaram, et al [12] and Armitt and Counihan [13] have discussed the conditions of similarity for correct modeling of atmospheric surface layers. Among the several criteria for similarity of model and prototype flows is geometric similarity. For the present case this means equality in the ratios of upstream boundary layer thickness δ to building height H or roughness length z_o for model and prototype. Values of these length ratios used in the wind tunnel study of Woo, et al [4] are summarized in Table 2. Of interest in the present comparison are values for condition No. 2, model No. 4 which were used in the wind tunnel investigation. These can be compared with corresponding values in the field study obtained by using the formula for estimating planetary boundary layer thickness given by Blackadar and Tennekes [14], viz.,

$$\delta = \frac{u^*}{4f} \tag{4}$$

If the value of u* at T6 of run No. 8407 from Table 1 (u* = 0.2218m/s) is taken as a near equilibrium value, and f is calculated from

$$f = 2\omega \sin \lambda \tag{5}$$

as $0.8133 \times 10^{-4} sec^{-1}$, then δ is estimated to be 682m. These values yield prototype length ratios of $H/\delta = 0.0047$ and $H/z_o = 457$ as compared with $H/\delta = 0.105$ and $H/z_o = 10.5$ for model. Thus noticeable dissimilarities appear in relative heights of surface roughness elements and the obstacle with respect to overall boundary layer thickness, and it is clear that the building extends into a much smaller part of the atmospheric boundary layer than does the model in its boundary layer. However both obstacles are in

the logarithmic layer governed by Equation (2), since Plate [15] estimates the thickness of δ_L of the logarithmic layer in a wind tunnel as $0.15\delta > H = 0.105\delta$, and Blackadar and Tennekes [14] give the atmospheric surface layer thickness, i.e., the patching height, as $0.04\delta > H = 0.0047\delta$. The ratios H/δ_L are unequal for model and prototype, but both upstream velocity profiles are logarithmic. The lack of geometric similarity is related to a corresponding dissimilarity in the turbulence structures of model and prototype flow fields.

The root-mean-square of the longitudinal component of velocity fluctuation u' is shown in Fig. 2 for the wind tunnel (solid curve) and the field (triangular and square points) as a function of nondimensional height z/H. The data are seen to become more disparate with increasing z/H, although some agreement is shown for $z/H < 2$. The disparity at large z/H is certainly explained by the difference in relative depth of the boundary layers, since the ratio of (δ/H) prototype to (δ/H) model is 22.38. This effect is illustrated by consideration of the field data point at $z/H = 6.5$, which would move to $z/H = 0.29$ if the δ/H ratios are taken into account. Thus the field data constitute only a very small segment of the u'/u^* curve for the whole boundary layer. Field data in the range $2.0 < u'/u^* < 2.5$ agree with other field and wind tunnel data for the constant shear stress layers, e.g., see Armitt and Counihan [12]. However, complete agreement of wake velocity profiles for prototype and model flows would not be expected in view of the turbulence dissimilarities at $z/H > 2$.

In the above discussion the heights of the atmospheric boundary layer and the surface layer have been crudely estimated. The assumed similarity between model and prototype layers at levels above the surface layer does not really exist. In view of the crudeness of the model implied by Eq. 1,

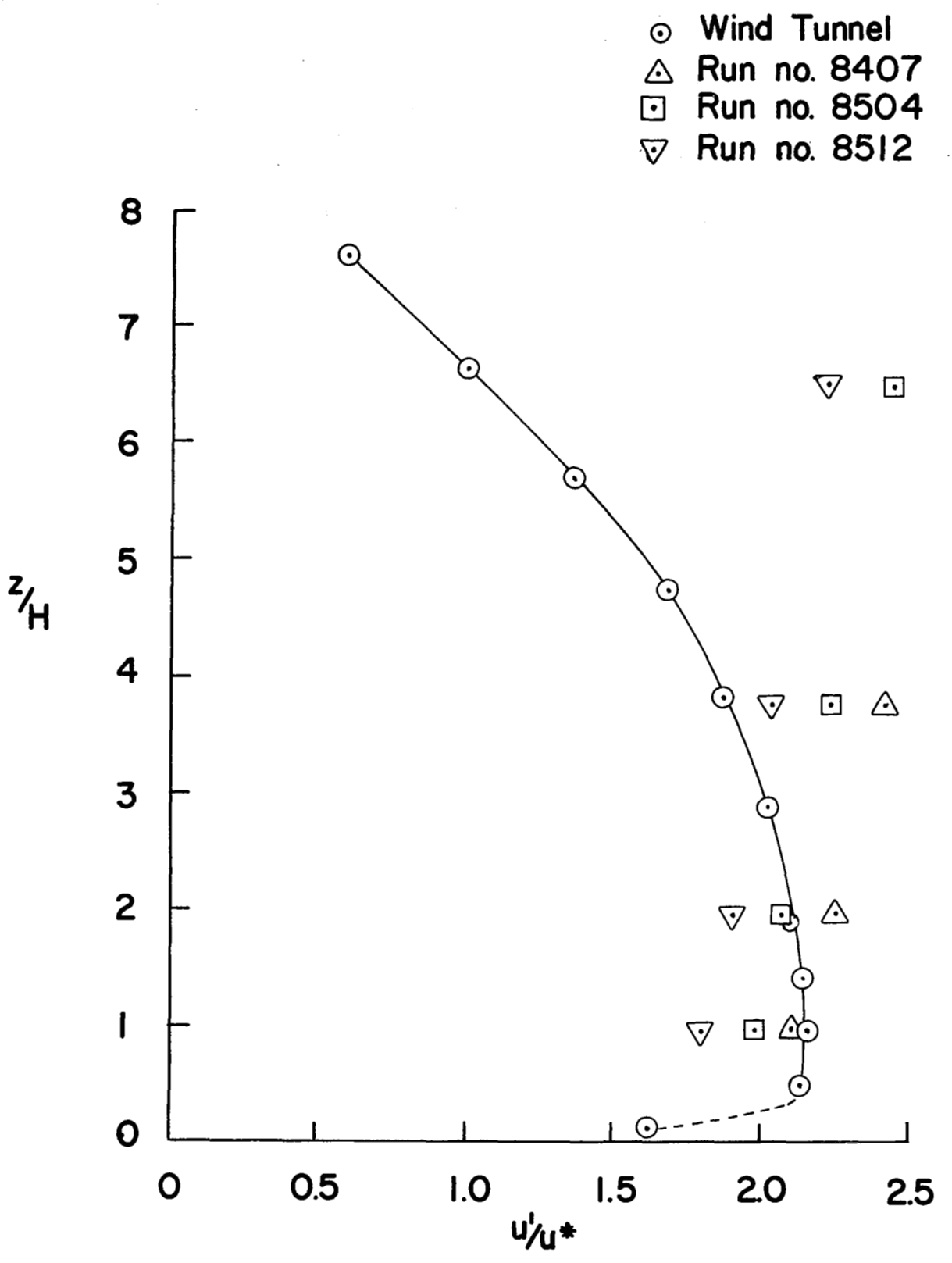

Fig. 2. Upstream Turbulence Profiles at x/H = -8.65, z/H vs u'/u*

Sundaram, et al [12] suggest that the height of the logarithmic layer δ_L should be considered in lieu of δ in the development of similarity parameters for the flow field around surface obstacles. Under this assumption the conditions for similarity become

$$(\frac{\delta_L}{H})_M = (\frac{\delta_L}{H})_P \tag{6}$$

and, as previously used,

$$(\frac{H}{z_o})_M = (\frac{H}{z_o})_P \tag{7}$$

An additional condition to assure that the effects of molecular viscosity are negligible, i.e., to assure an aerodynamically rough tunnel wall, is

$$(\frac{u^* z_o}{\nu})_M \geq 3 \tag{8}$$

Combination of Equations (2), (6) and (8) leads to

$$(\delta_L)_M \geq \frac{3\nu}{k U_M} (\frac{\delta_L}{z_o})_P \ln (\frac{\delta_L}{z_o})_P \tag{9}$$

Equation (9) gives δ_L = 0.32m for the minimum thickness of the logarithmic layer in the wind tunnel. Figure 2 shows that $\delta_L \simeq$ 2H = 0.128m for the actual wind tunnel flow. However, the required δ_L obtained from Equation (9) could be reduced by running the wind tunnel at a higher speed U_M. In order to satisfy Equations (6) and (7), the model should have a height H of 1.5 cm, and the wind tunnel wall should have a roughness length of 0.0000355m. These values are based on δ = 682m and δ_L = 0.04δ = 27.28m, and these values could conceivably be larger by a factor of three or four, thus increasing the model height H to the value actually used (6.4 cm). However, calculating δ from Equation (4)

using the data for u* from Table 1 (T6), a factor of two, i.e., $\delta \simeq 1400$m, is a more reasonable upper limit for the field runs listed.

In general, the similarity conditions of Sundaram, et al [12] require a higher tunnel speed, a smaller model size and a smoother tunnel wall. Since the wind tunnel conditions actually used by Woo, et al [4] to model the field conditions studied by Frost and Shahabi [8] are not strictly similar, some disparity is to be expected in the wake profiles. On the other hand, at least qualitative similarity of wake profiles should be expected owing to the approximately equal and constant (with height) upstream values of u'/u* in the logarithmic layer and equal power law exponents n for upstream velocity profiles.

CHAPTER 4

COMPARISON OF WAKE VELOCITY PROFILES

The effect of the building or model on the upstream velocity profile is studied in this chapter by comparison of field and wind tunnel data presented graphically in non-dimensional form. Figure 3 shows the wind tunnel velocity profile for Test Condition 2 upstream of Model 4 compared with field profiles at tower T1 for Runs 8407, 8504 and 8512. In this figure the reference velocity, U_r, used is that at tower T1, level 4, i.e., at z/H = 6.5. Data for Run 8407 agree almost perfectly at all levels except z/H = 1.94. Data for Run 8504 make up a slightly fuller profile but are in excellent agreement, and those for Run 8512 indicate a slightly straighter profile.

Profiles at tower T4 are compared in Fig. 4 for the two field runs 8407 and 8504. The profile of Run 8504 appears to be slightly shifted to the right, which may indicate some unaccountable external effect which has increased the layer's momentum at every level over that observed in Run 8407. The possibility that this effect is produced by a change in height of natural cbstacles (hedges and trees) upwind of the simulated building associated with the eight-month difference in time between Run 8407 and Run 8504 must be eliminated because of the very good agreement at level 4 of the data of Run 8512 with the earlier data.

The enhancement of momentum at level 4 is, however, also observed for Run 8407 far downwind in the wake, i.e., at tower T6. This may be inferred from a comparison of data for Runs 8407 and 8512 in Figs. 4 and 6. Unfortunately, good data at level 4 tower T6, is not available, but it is clear that data for 8407 follows 8512, and thus that significant

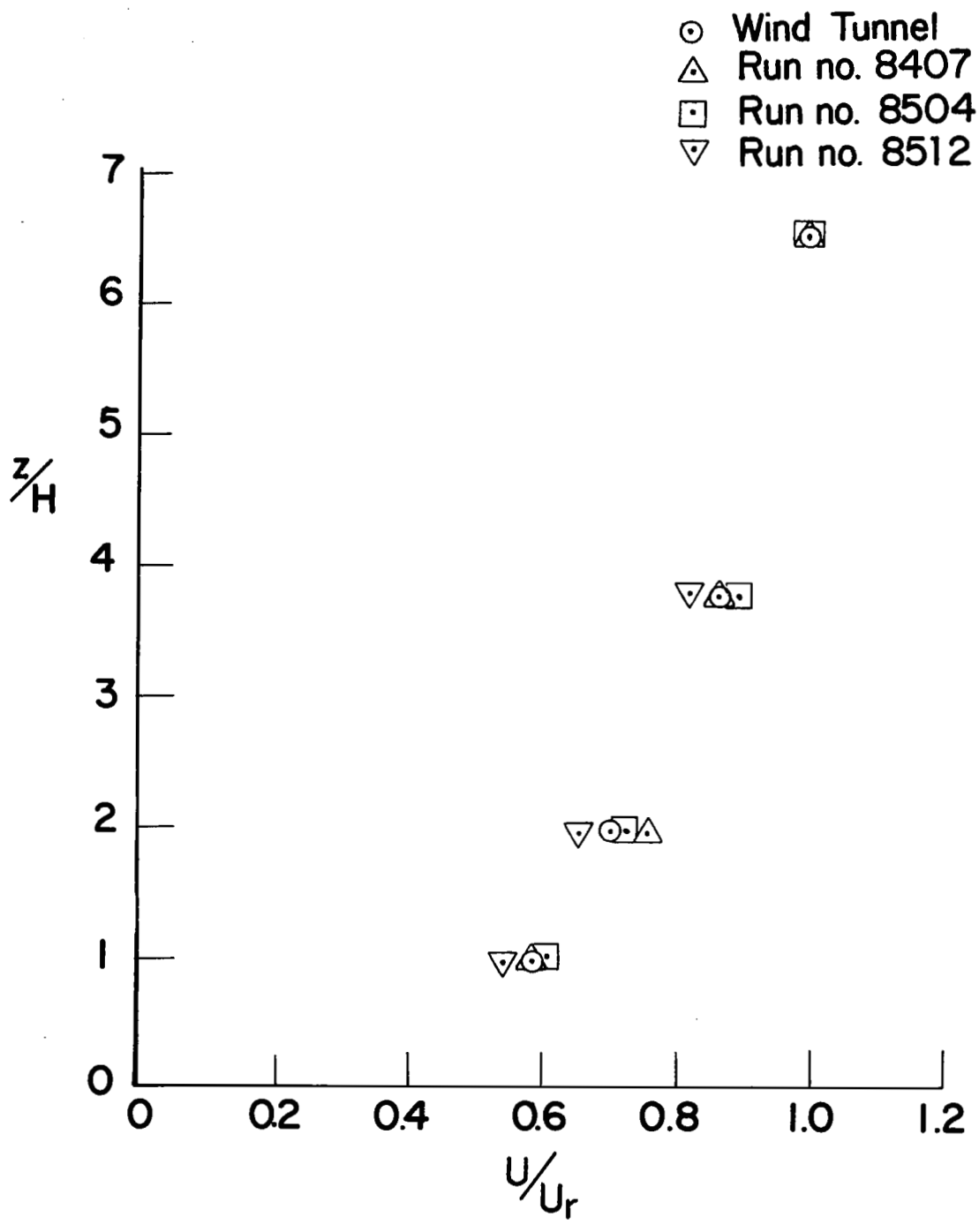

Fig. 3. Upstream Wind Profiles at x/H = -8.65

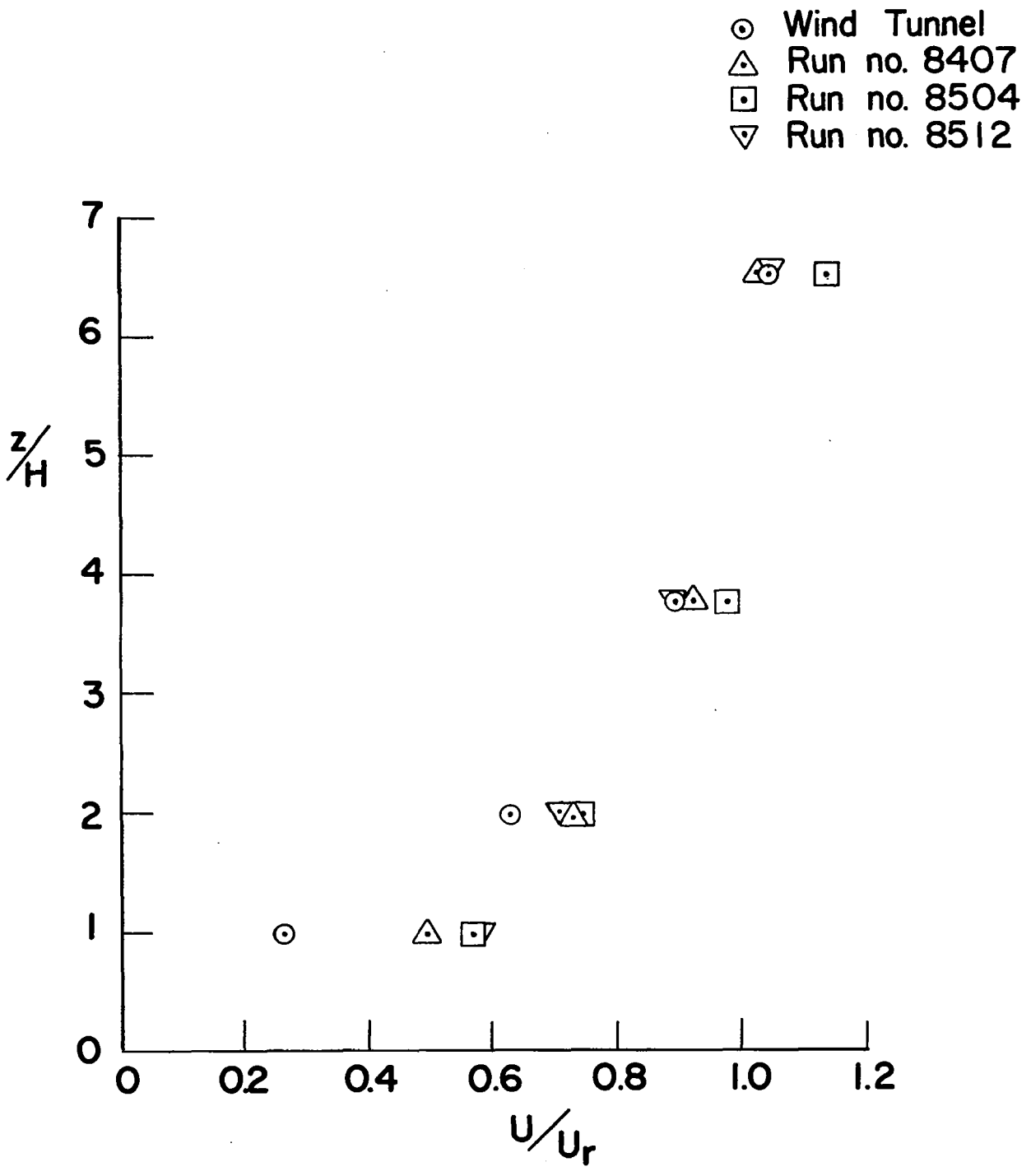

Fig. 4. Wind Profiles Upstream of Reattachment at x/H = 4.88

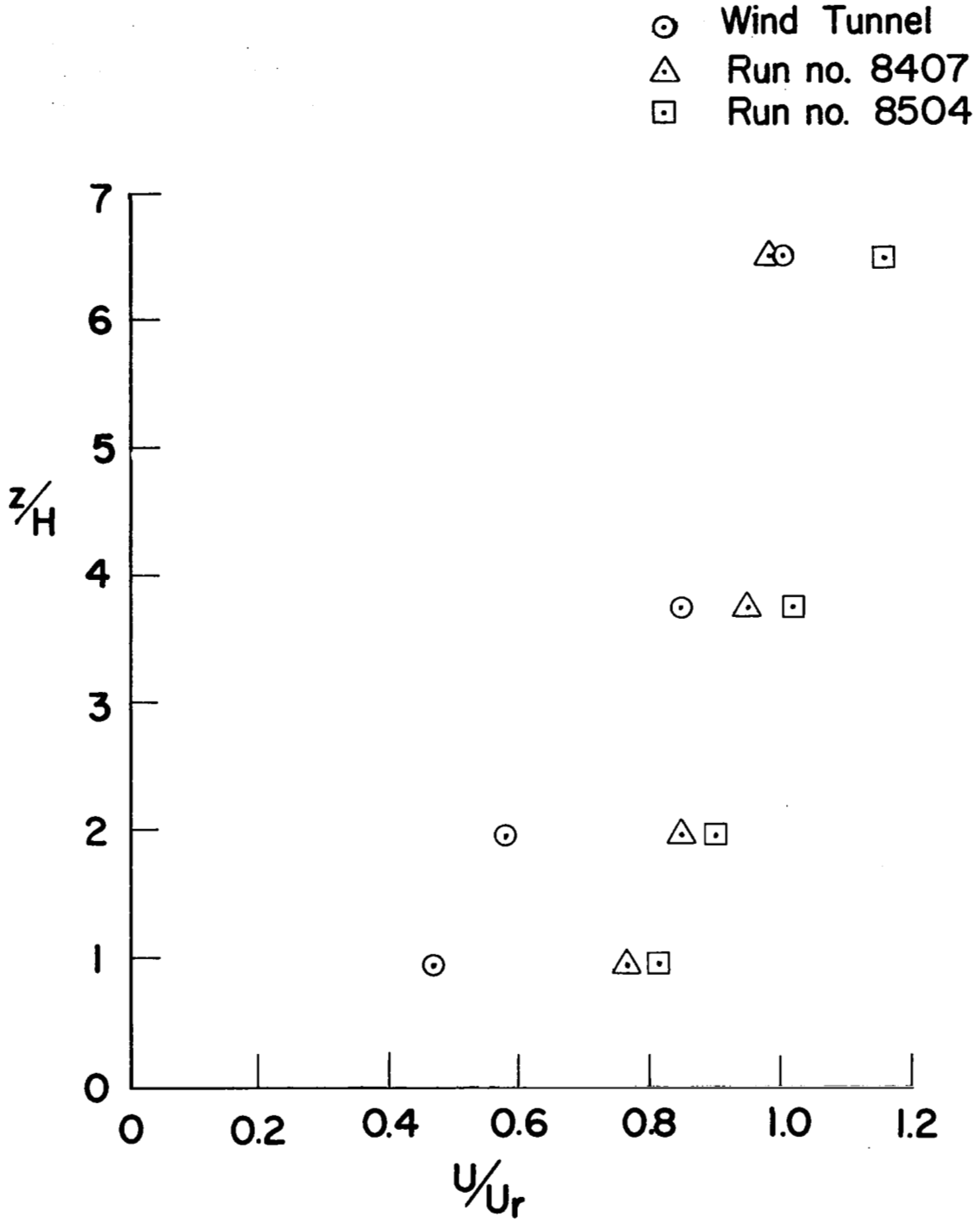

Fig. 5. Wind Profiles Downstream of Reattachment at x/H = 16.44

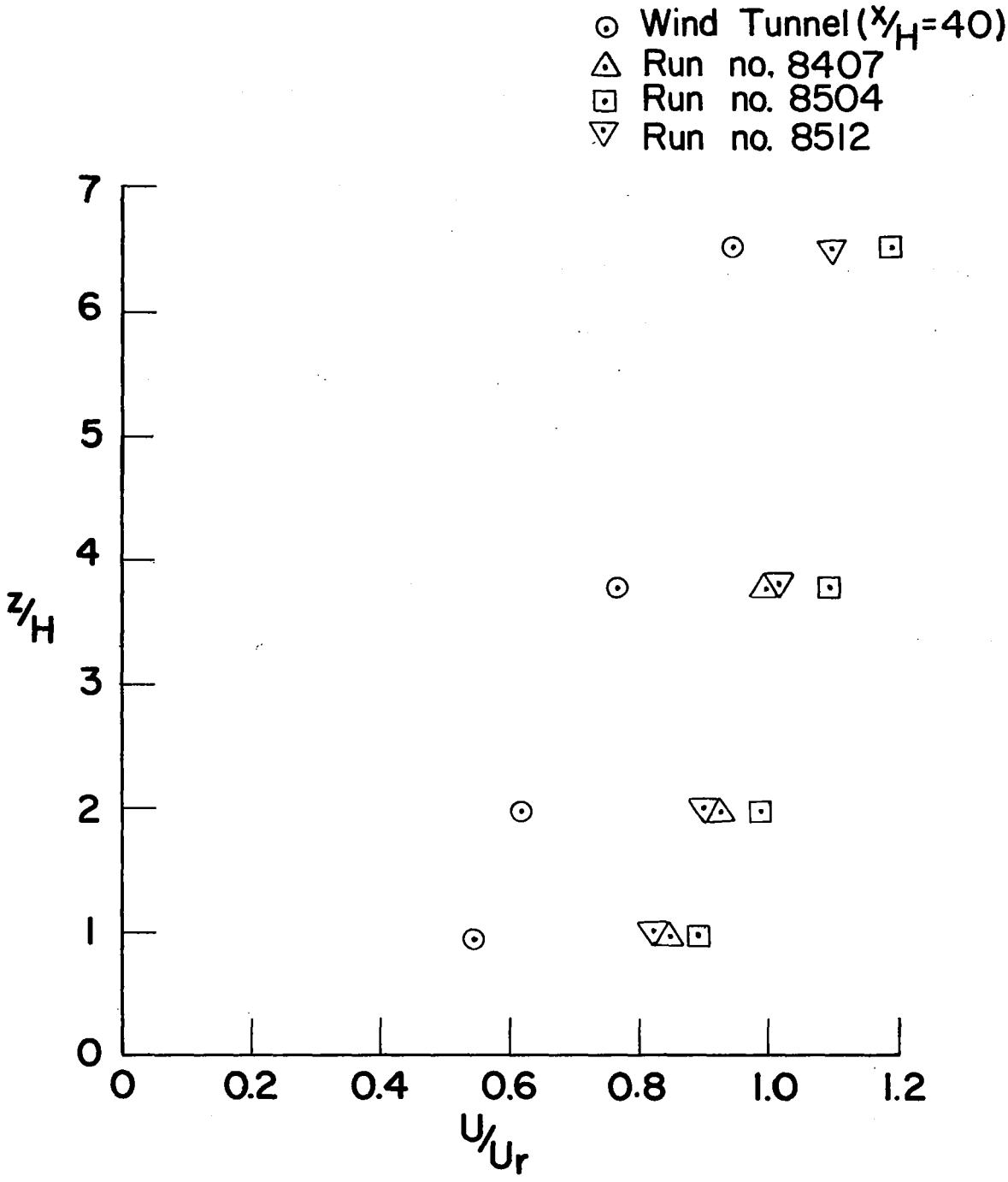

Fig. 6. Wind Profiles Far Downstream at x/H = 43.94

momentum enhancement is evident at tower T6 for both of these runs, as well as Run 8504.

A rough estimation of momentum flow per unit width MOM is obtained by evaluating the integral

$$MOM = \int_0^{20.88} U^2 dz \qquad (10)$$

for Run 8504. This integral is evaluated at $998m^3/s$ at T6 compared to $629m^3/s$ at T1. This is an increase of 59% over the upstream momentum for the layer defined by $0 < z < 20.88m$. However, the wind tunnel data applied to the corresponding model layer yields $47m^3/s$ at T6 compared with $57.3m^3/s$ at T1, i.e., a momentum decrease of 18%. Since a momentum decrease is expected, the validity of the field data is suspect. However, in view of the conclusions reached in Chapter 2 of this report, the upstream field profile is not an equilibrium profile, whereas the wind tunnel profile is a fully developed profile, i.e., the field profile is in the process of receiving horizontal momentum from the layer above it at the time it passes over the simulated building (and loses momentum) and the process of momentum addition continues in the wake of the building with a condition of near equilibrium being achieved at station T6. Thus the fullness of the profile at T6 would be present at T1 also if equilibrium had obtained there. Data from other runs were used to evaluate the momentum integral of Equation (10), and the results are presented in Table 3. These data provide convincing evidence that the wind profiles at T1 are not equilibrium profiles.

The possibility that the apparent increase in momentum is a momentum decrease at T1 associated with the presence of the building 8.65 building heights downstream of T1. Based on the measurements of Rider [16] it is

estimated that this effect could indicate an anomalous increase of as much as five percent. However, values shown in Table 3 indicate much larger increases.

Table 3. Momentum Integral Evaluation

(Units are m^3/s)

Run No.	MOM at T1	MOM at T6
8501	554	916
8502	660	919
8503	650	1007
8512	421	617
8407	334	428
8408	288	410

Figures 3 through 6 show what is though to be a continuing adjustment of field wind profiles to local surface roughness combined with a recovery from the retardation associated with the passage of the air over the building. Since the wind tunnel profile is merely returning to equilibrium and its z_o/δ value is greater than the corresponding field value, the wind tunnel profile shown in Fig. 6 does not match that measured in the field for a much smaller relative roughness. The disparity between model and prototype wake profiles is illustrated qualitatively in Fig. 7 where Equation(1) is used to determine equilibrium profiles using $n = 0.27$ for the wind tunnel and $n = 0.13$ for the field. The latter exponent is reasonable for $z_o = 0.7$ cm (e.g., see Plate [15], p. 41). Thus qualitative prediction of the downwind wake profiles ($x/H \simeq 40$) is possible a priori, given only the values of z_o for the prototype and model.

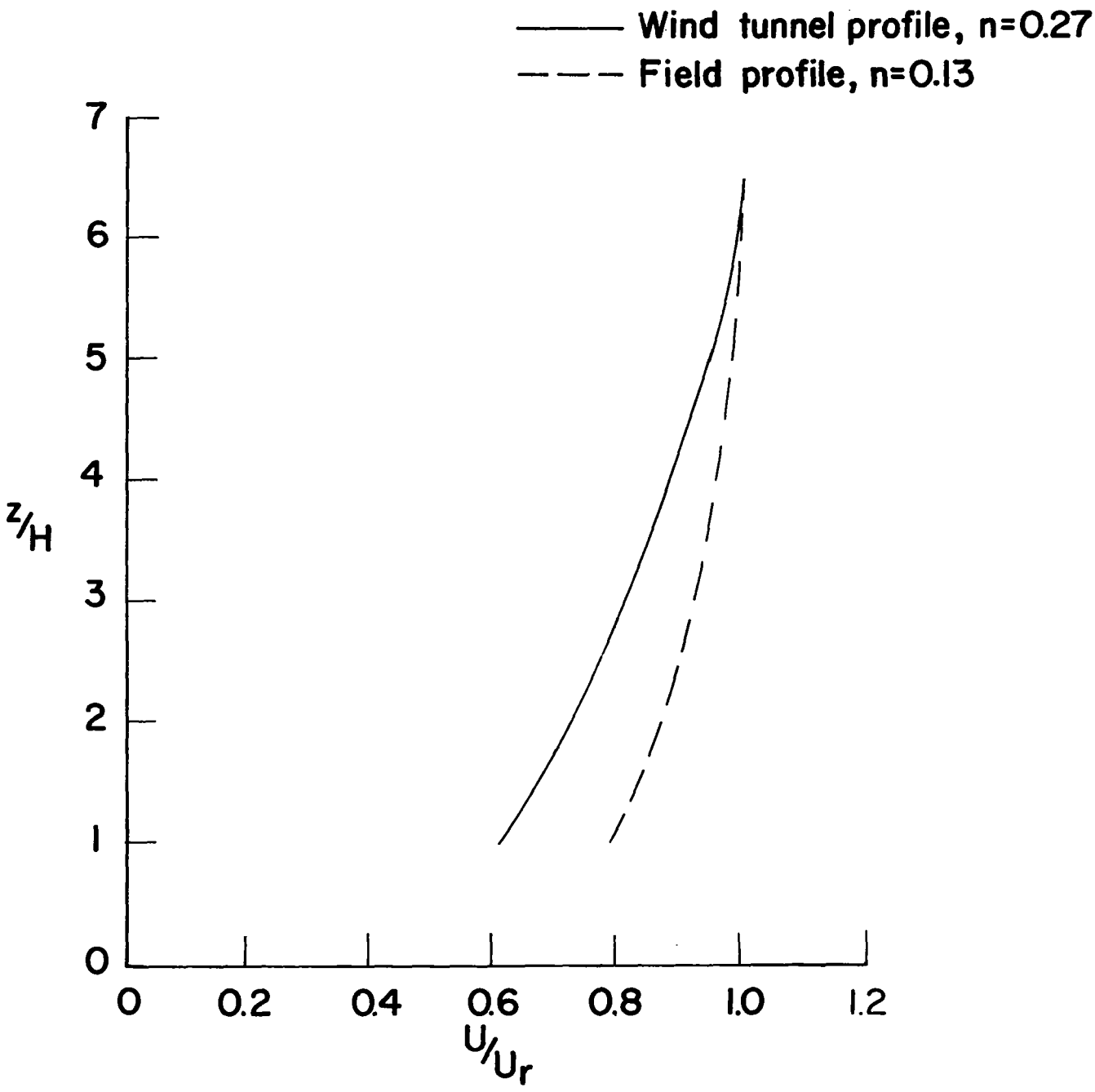

Fig. 7. Estimated Wind Profiles far Downstream of Building

The relative effect of the obstacle on the flow may also be observed in Figs. 3 through 6. A very significant retardation is noted in the wind tunnel wake, but almost no retardation is observed in the field profiles. Accompanying the greater retardation is a 75% higher velocity gradient at the lower levels which should lead to greater turbulence levels in the wind tunnel wake. These observations can be explained by the greater value of H/δ in the wind tunnel flow. Figure 8, which is based on the correlations of Good and Joubert [7], shows qualitatively that the effect of increasing H/δ is to increase C_D for the obstacle. The graphs indicate that the use of a model with H/δ greater than the prototype and with H/z_o less than the prototype would produce a larger C_D, and hence a greater momentum deficit and turbulence excess would be expected.

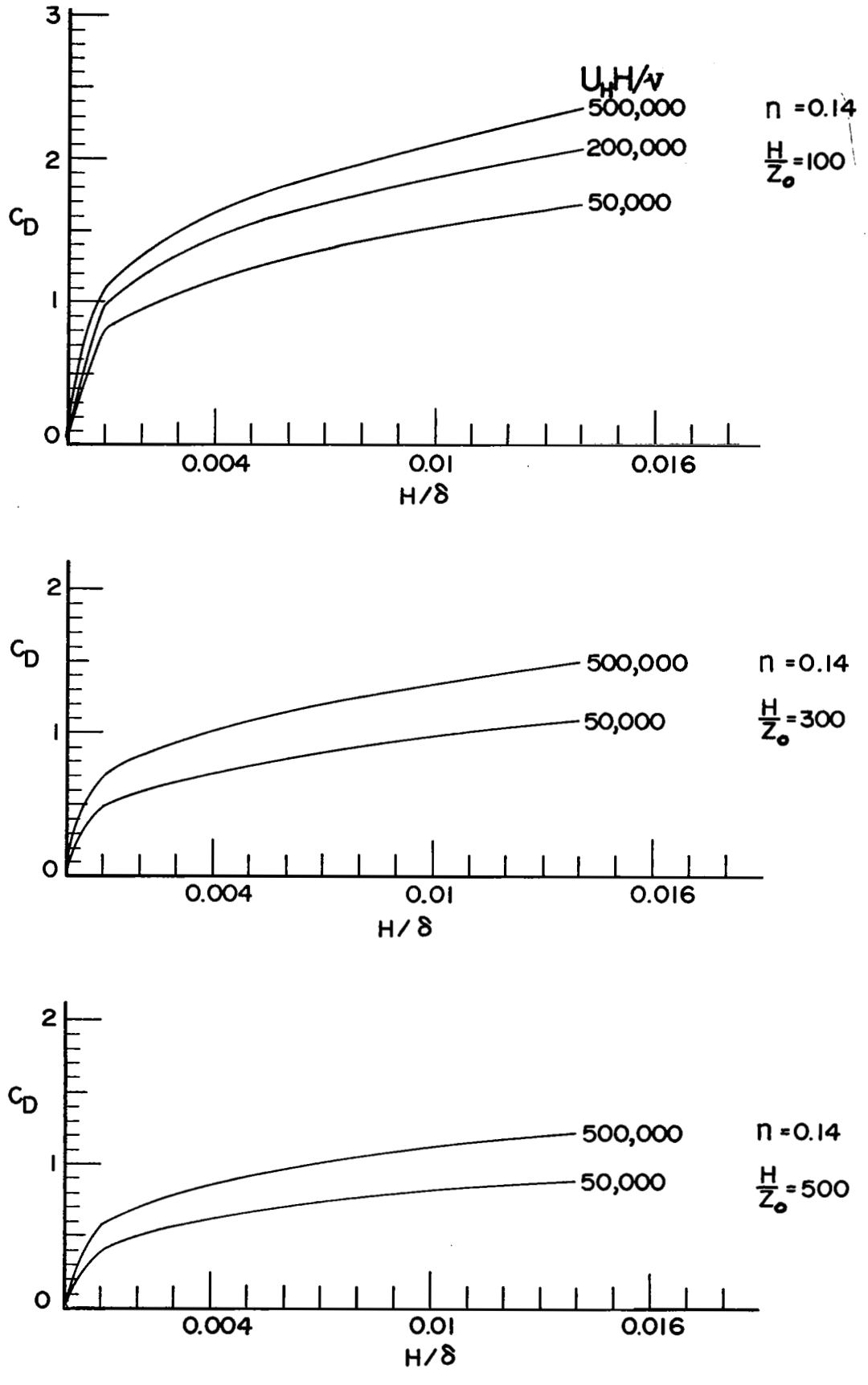

Fig. 8. Effect of Relative Obstacle Height

CHAPTER 5

COMPARISON OF WAKE TURBULENCE PROFILES

Figure 2 was used to show the comparison of upstream turbulence distribution. Figures 9 through 15 extend the comparison to wake profiles. Figures 9 through 12 show the RMS value of longitudinal turbulence u' nondimensionalized with reference mean velocity U_r. The upstream profiles for model and prototype shown in Fig. 9 do not intersect at any point. This is a different behavior than previously exhibited in Fig. 2 for u'/u* profiles using the same turbulence data. On the other hand, the field data plotted in Fig. 9 are in close agreement. The same apparent independence of field and wind tunnel data is observed at the other stations shown in Figs. 10 through 12. The near equilibrium profiles of Fig. 12 are very close to the starting profiles of Fig. 9.

The response of the flow to the obstacle shown in Fig. 10 is stronger for the model than for the prototype, e.g., u' increases 70% for the model and 15% for the prototype at level 2. This effect agrees with the difference in velocity gradient observed in Fig. 4 for the same station, i.e., the wind tunnel velocity gradient is 75% higher than the field gradient in the lower part of the layer, which implies a correspondingly higher relative turbulence production for the wind tunnel layer just downstream of the obstacle. Another point of agreement is the previously noted difference in momentum flow, i.e., the greater increase in velocity gradient observed in Fig. 4 is associated with a greater momentum loss, which implies a greater relative drag force on the obstacle. A greater relative

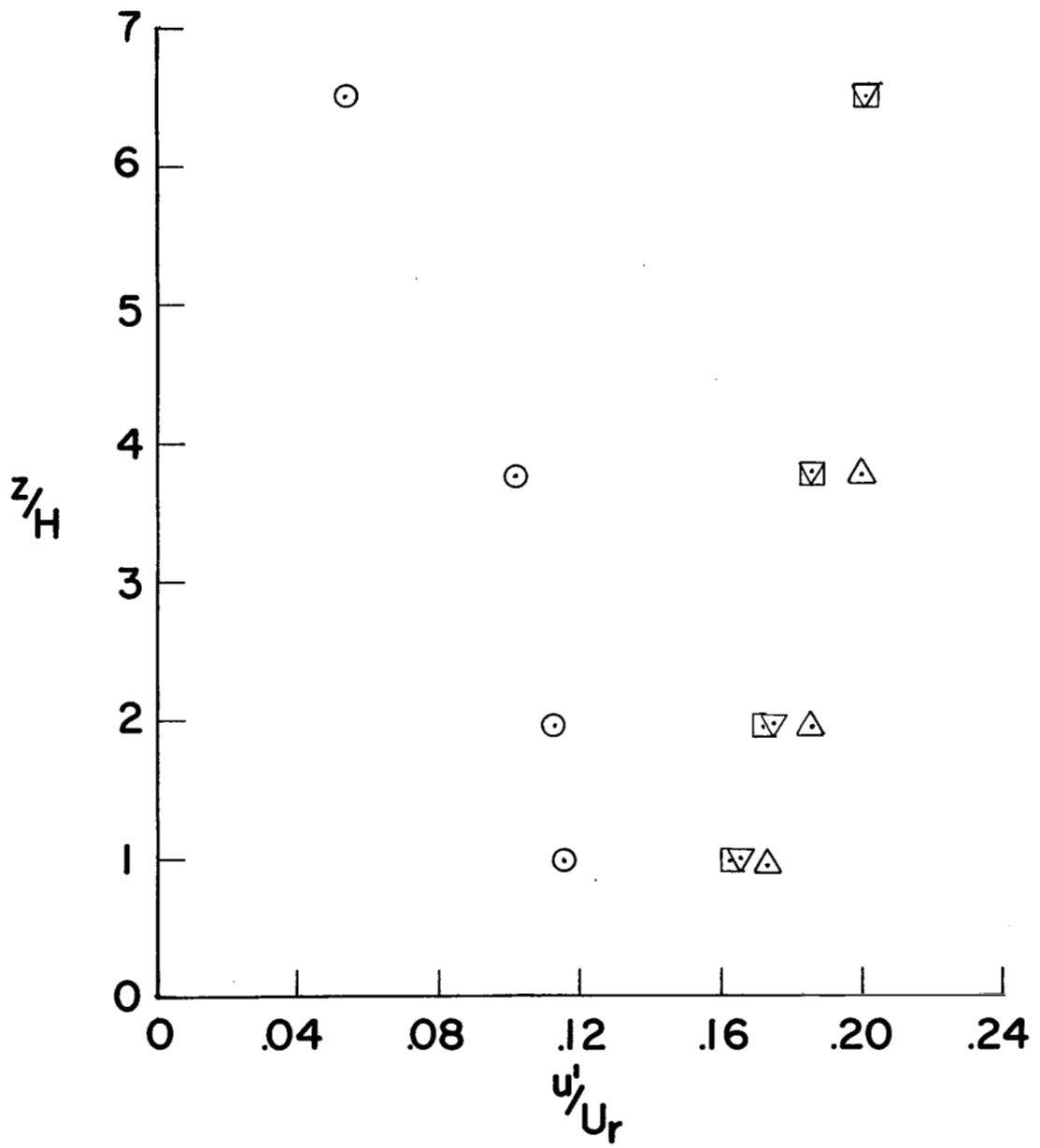

Fig. 9. Upstream Turbulence Profiles at x/H = -8.65, z/H vs. u'/U_r

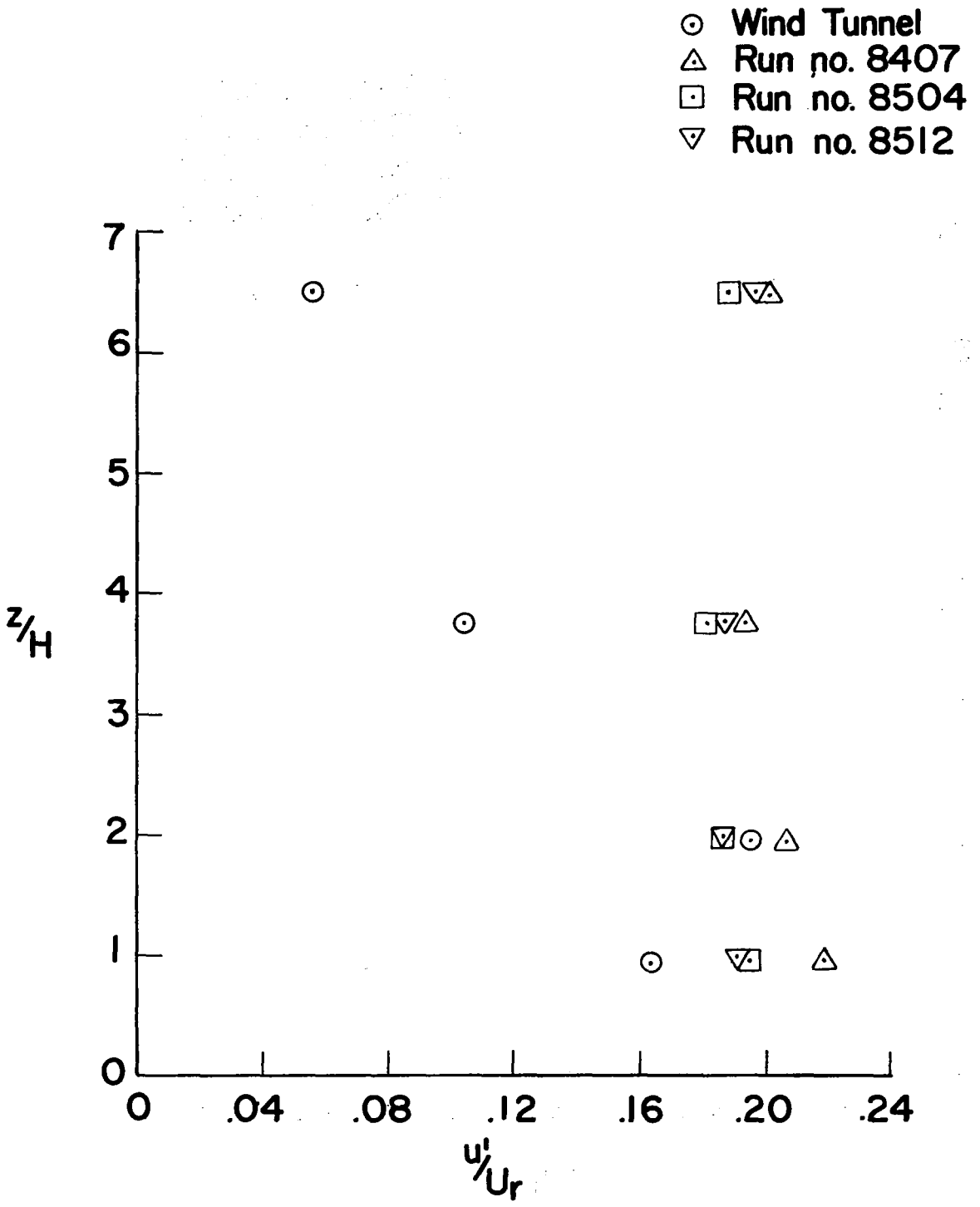

Fig. 10. Turbulence Profiles Upstream of Reattachment at x/H = 4.88

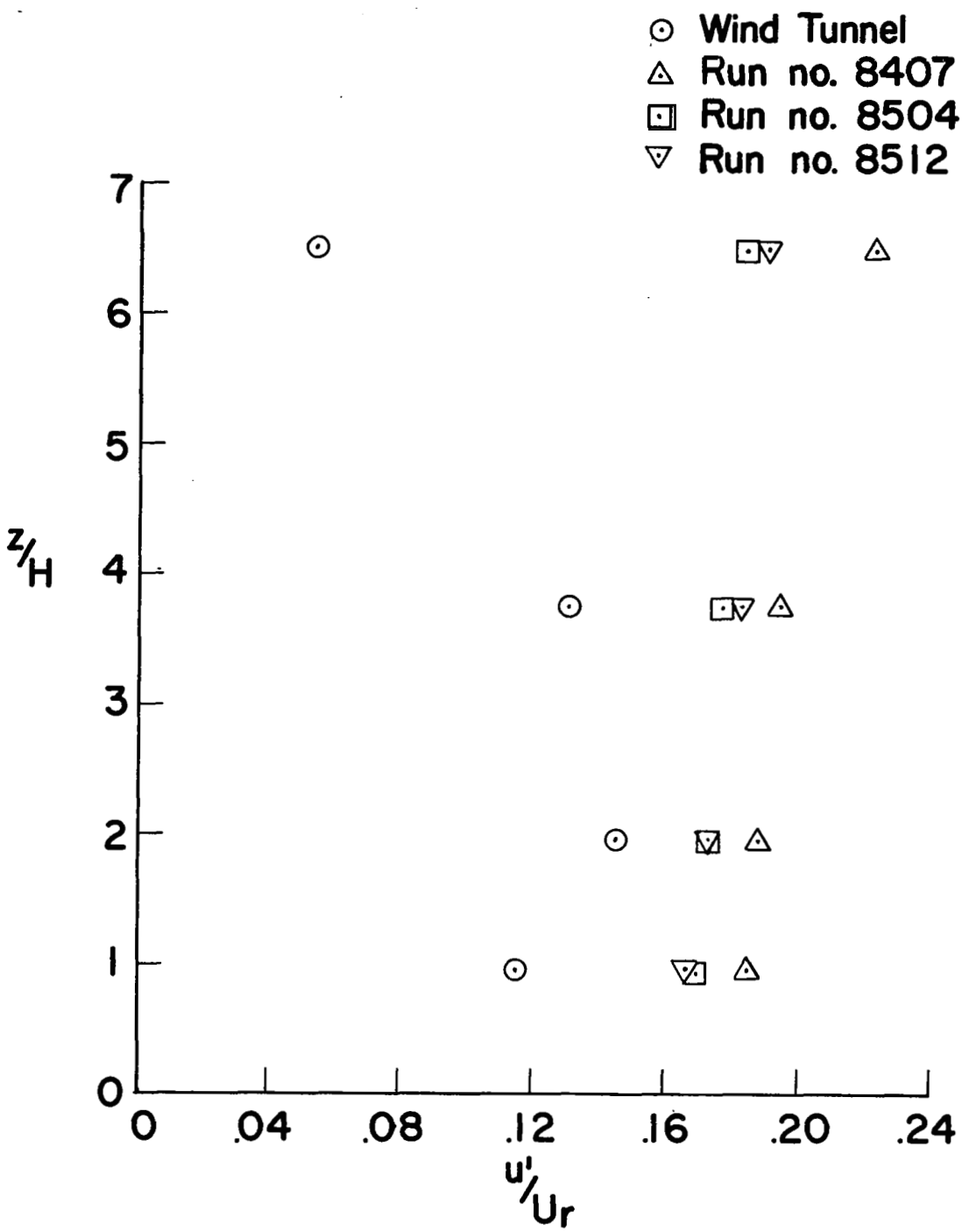

Fig. 11. Turbulence Profiles Downstream of Reattachment at x/H = 16.44

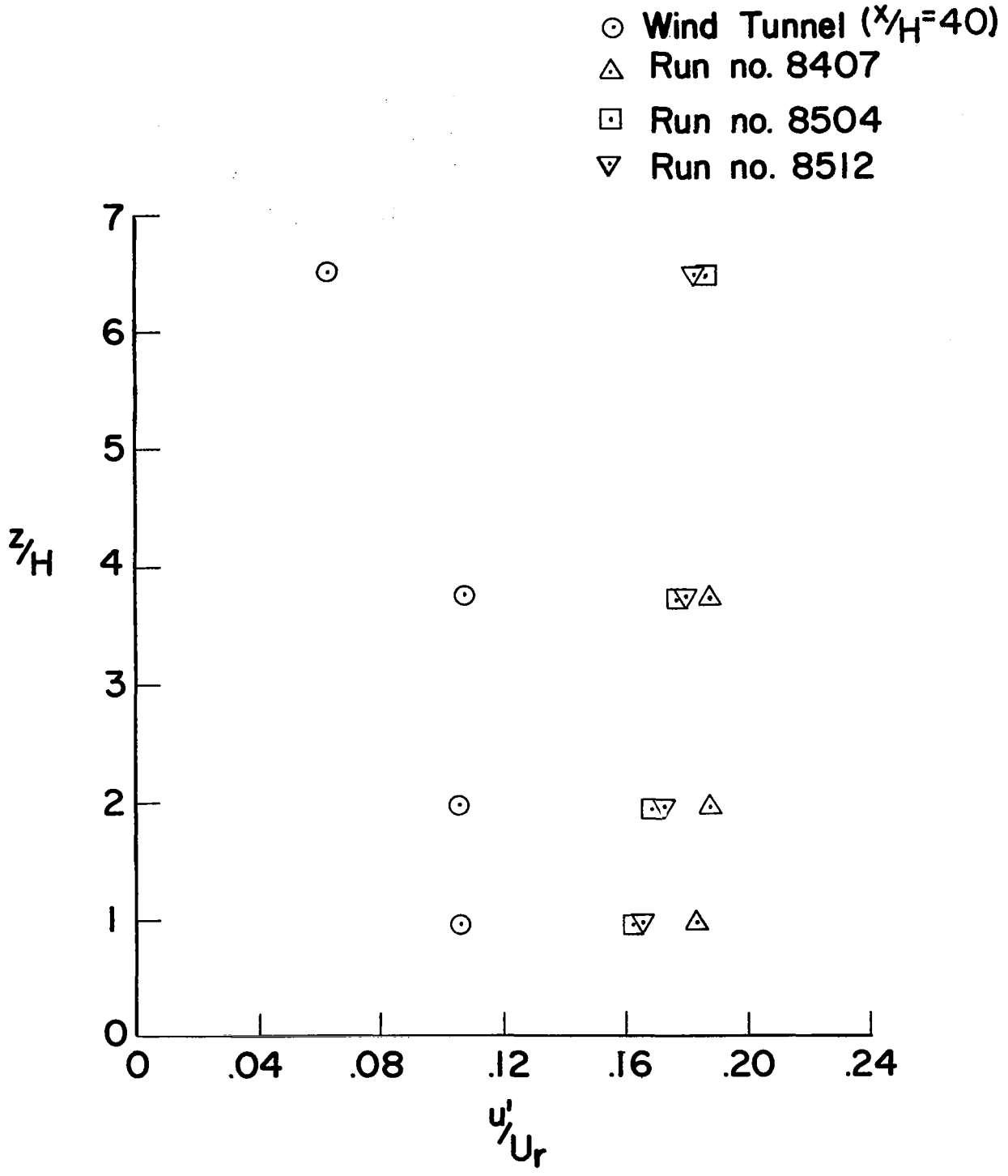

Fig. 12. Turbulence Profiles Far Downstream at x/H = 43.94

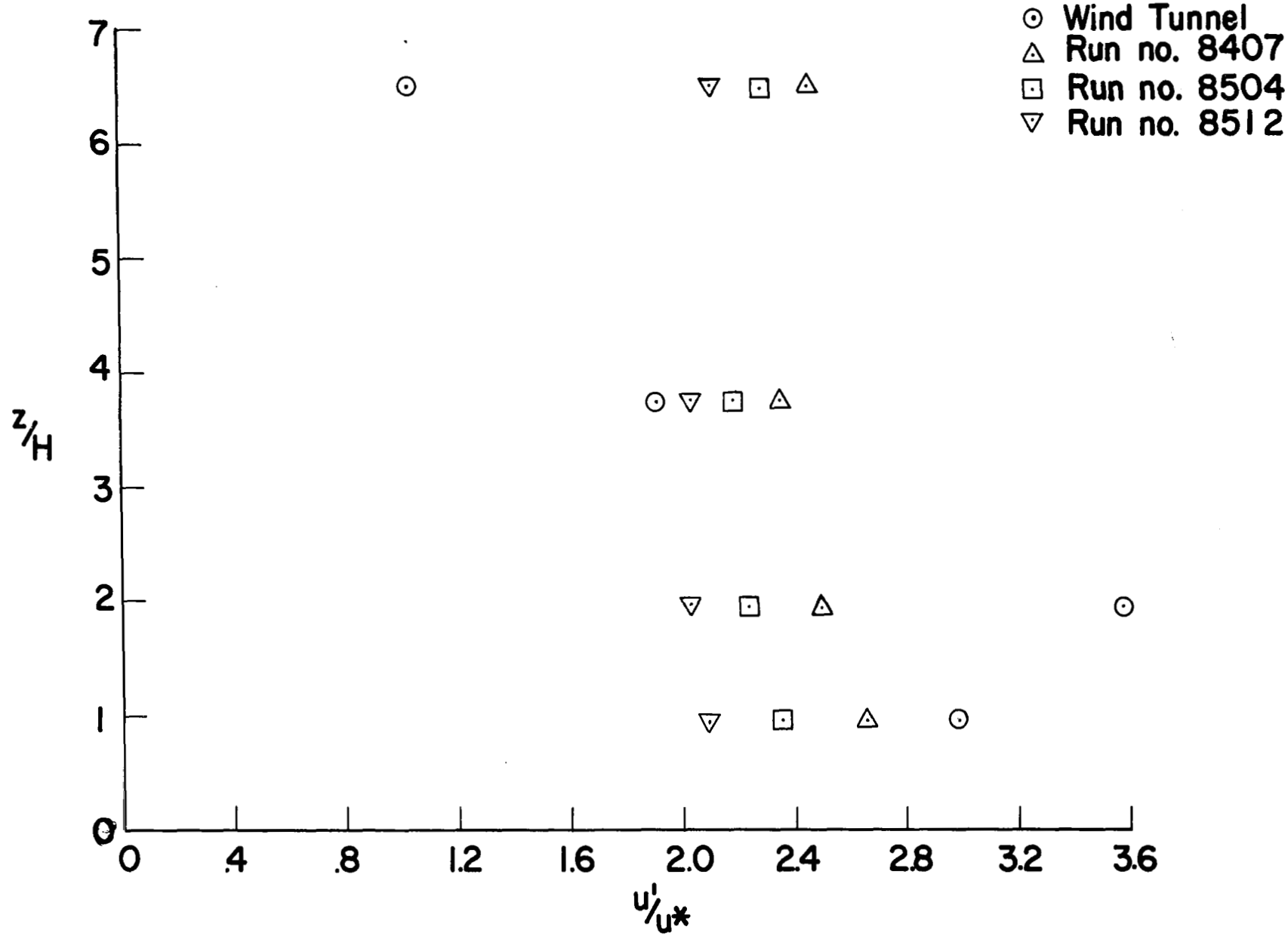

Fig. 13. Turbulence Profiles at x/H = 4.88

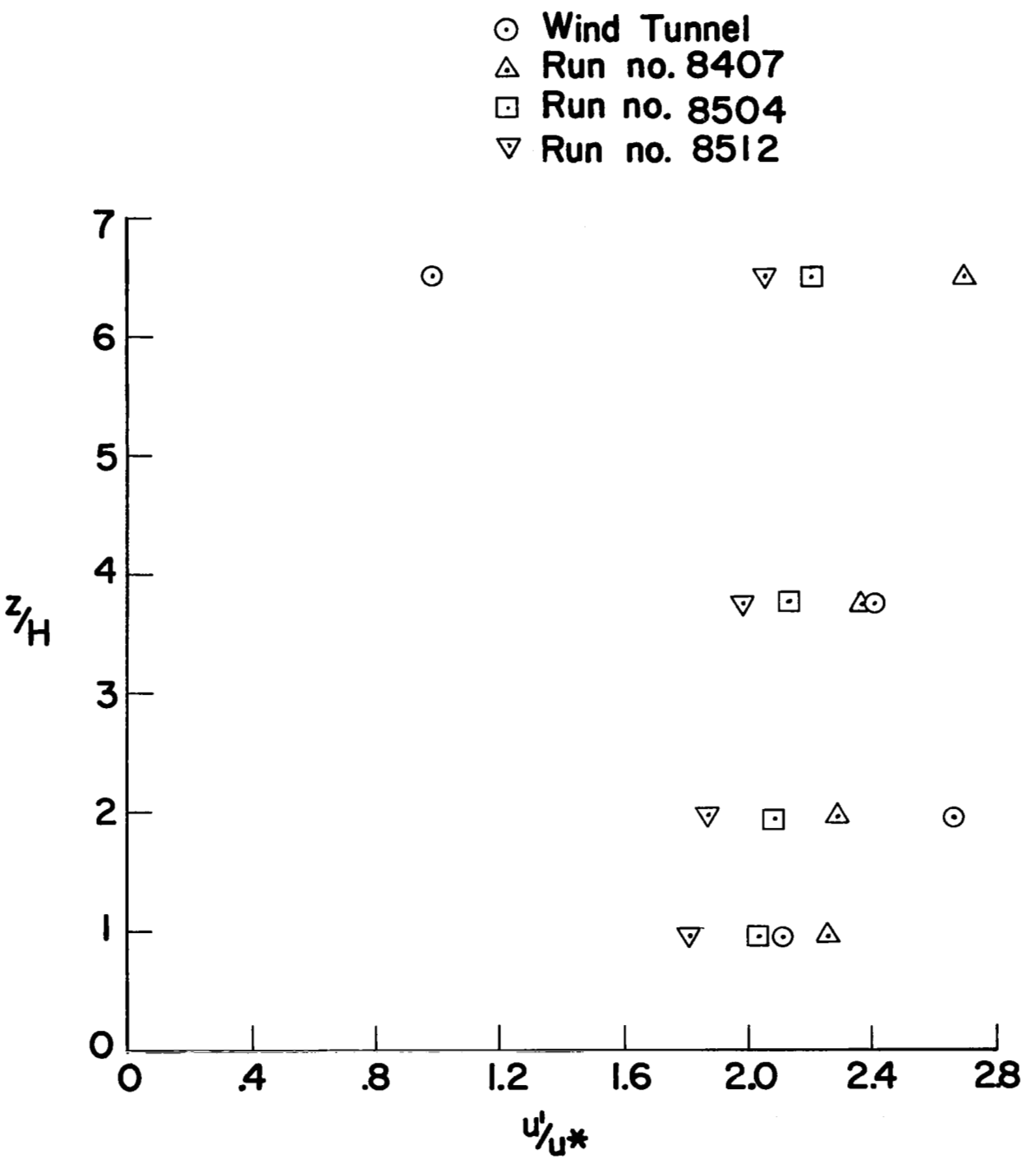

Fig. 14. Turbulence Profiles at x/H = 16.44

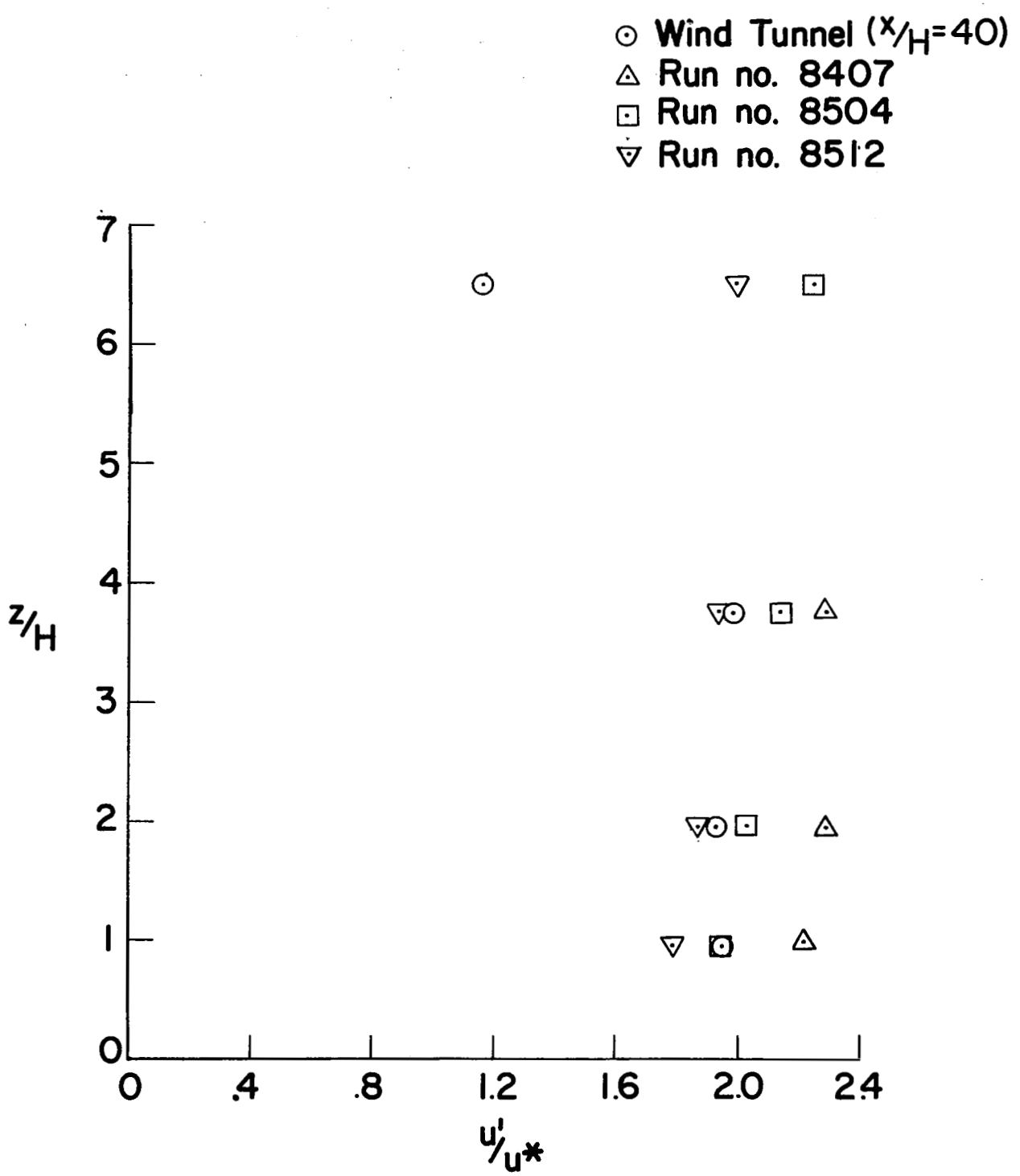

Fig. 15. Turbulence Profiles at x/H = 43.94

drag force is expected for the greater value of H/δ present in the wind tunnel as was shown in Fig. 8.

Turbulence wake profiles, non-dimensionalized with friction velocity, are shown in Figs. 13 through 15. More scatter of field data points is observed in these graphs, but a better mingling of wind tunnel and field points is noted. This is particularly true at the farthest downstream station as shown in Fig. 15. Here wind tunnel data for levels one through three agree almost perfectly with the field data.

CHAPTER 6

COMPARISON WITH WAKE THEORY

An alternative to direct comparison of velocity profiles is a comparison of model and prototype profiles with those obtained from wake theory. One way this can be done is to calculate an approximate value of the parameters introduced by Counihan, et.al. [3], which are called ζ and η herein, and are defined as

$$\eta = \frac{z}{H} \left(\frac{KX}{H}\right)^{-\frac{1}{n+1}} \tag{11}$$

and

$$\zeta = -\frac{\Delta U x}{U_H H} \tag{12}$$

with the constant K calculated from

$$K^{-1} = \frac{U_H}{2k\ u^*} \tag{13}$$

The velocity deficit ΔU is defined by Frost and Shahabi [8] as the loss in momentum per unit mass at a given height, i.e., U at a downstream station minus U upstream of the building at the same distance z above the ground. The wind tunnel profiles shown in Fig. 16 are based on the foregoing definition of ΔU. However, the field profile, indicated with open square points, is based on defining ΔU as U at T5 minus U at the same level of T6. This is done since the profile at T1 is apparently not fully developed, so that its use would result in $\Delta U > 0$ in the wake. Although the alternate definition of ΔU is necessary and useful, it is impossible to draw conclusions regarding the comparison of the field

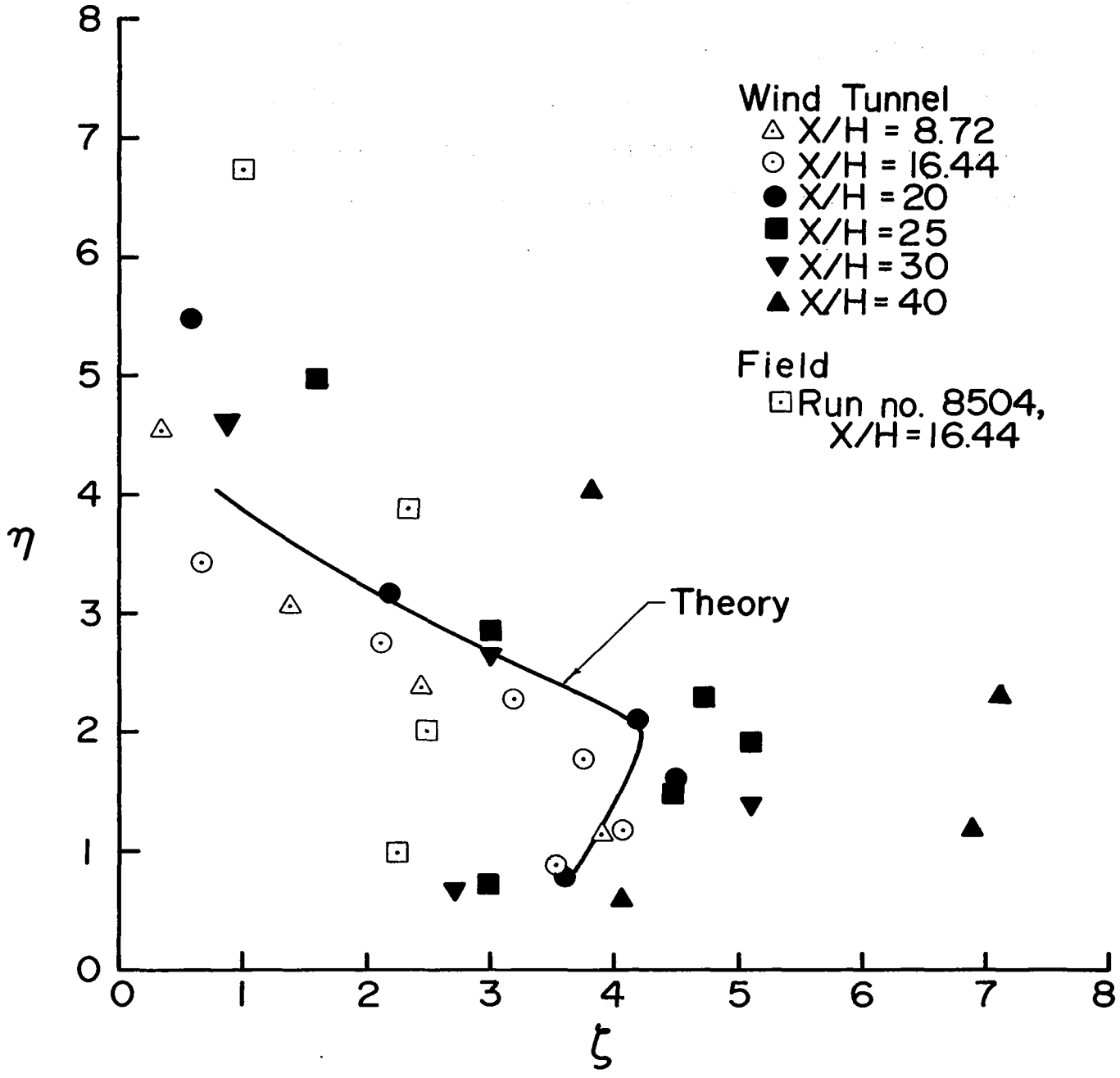

Fig. 16. Comparison of Wake Profiles with Theory

profile with theory or with the wind tunnel profiles in the deficit form.

The wind tunnel measurements shown in Fig. 16 are qualitatively similar to those presented by Counihan, et.al. [3]. A theoretical curve, calculated by the methods of Counihan, et.al. [3] is also included in Fig. 16 for comparison with wind tunnel wake profiles. Approximate agreement of theory and measurement is observed for x/H = 20 and below. A large disparity is noted at x/H = 40. Below $\eta \simeq 1.5$ the correlation is extremely good up to station x/H = 25, indicating a self-preserving ζ-η relation within these limits. Above $\eta \simeq 1.5$ the ζ-η profiles tend to spread somewhat, so that the profile depends on x/H. Attempts are being made presently to modify the calculated parameters to produce a better correlation.

Attempts to correlate data for the purpose of predicting the wake velocity and turbulence profiles have been investigated. Some results are presented in the appendix. Correlations of this sort should be very useful tools in predicting full scale wake behavior.

CHAPTER 7

CONCLUSIONS

Several conclusions may be drawn from a preliminary comparison of field data taken from the MSFC-ABLF and wind tunnel data obtained from the CSU-MWT. Similarity conditions require a higher tunnel speed, a smaller model size and a smoother wind tunnel wall. The observed disparity in wake wind profiles stems from differences in δ/z_o which are associated with differences in power law exponents. The percent turbulence increase generated by the model (70%) is larger than the corresponding u' increase (15%) developed by the prototype; this difference may be accounted for by the greater value of H/δ present in the wind tunnel. Field turbulence profiles, u'/u^* as a function of z/H, are roughly predictable from model data at $x/H = 44$ provided $z/H < 3$. Wake theory agrees approximately with wind tunnel data for $x/H \leq 20$. A self preserving wind tunnel wake, indicated by a good correlation of data in a ζ-η plot exists for $\eta \leq 1.5$ and $x/H < 25$.

Further work is needed to achieve adequate data comparison. Suggested studies would include the reverse flow case ($\theta = 0°$), v' and w' turbulence components, velocity deficit decay, turbulence decay and spectra, three dimensional effects, recirculation zone data, and the perturbation of non-equilibrium flow.

REFERENCES

1. Fichtl, G.H., Camp, D.W. and Frost, W., "Sources of Low-Level Wind Shear Around Airports, " J. Aircraft, Vol. 14, 1977, pp. 5-14.

2. Frost, W., "Review of Data and Prediction Techniques for Wind Profiles around Manmade Surface Obstructions," AGARD Conference Proceedings No. 140, Flight in Turbulence, 1973.

3. Counihan, J., Hunt, J.C.R., and Jackson, P.S., "Wakes behind Two-dimensional Surface Obstacles in Turbulent Boundary Layers," J. Fluid Mech., Vol. 64, 1974, pp. 529-563.

4. Woo, H.G.C., Peterka, J.A., and Cermak, J.E., "Wind Tunnel Measurements in the Wakes of Structures, " NASA CR-2806, NASA/Marshall Space Flight Center, Al, 35812, 1977.

5. Oka, S. and Kostic, Z., "Flow Field Past a Single Roughness Element in Channel of Rectangular Cross-Section," Heat and Mass Transfer in a Boundary Layer, Vol. 1, 1972, pp. 425-435.

6. Mueller, Thomas J. and Robertson, James M., "A Study of the Mean Motion and Turbulence Downstream of a Roughness Element, " Modern Developments in Theoretical and Applied Mechanics, Vol. 1, 1963, pp. 326-340.

7. Good, M.C., and Joubert, P.N., "The Form Drag of Two-dimensional Bluff Plates Immersed in Turbulent Boundary Layers," J. Fluid Mech., Vol. 31, Part 3, 1968, pp. 547-582.

8. Frost, W. and Shahabi, A.M., "A Field Study of Wind Over a Simulated Block Building," NASA CR-2804, NASA/Marshall Space Flight Center, Al, 35812, 1977.

9. Frost, W., Fichtl, G., Connell, J.R. and Hutto, M.L., "Mean Horizontal Wind Profiles Measured in the Atmospheric Boundary Layer about a Simulated Block Building," Boundary Layer Meteorology, Vol. 11, 1977, pp. 135-145.

10. Sacre, C., "Experimental and Theoretical Study of Air Flow over Hill," Proceedings of the Third U.S. National Conference on Wind Engineering Research, Univ. of Florida, Feb. 26-Mar. 1, 1978, pp. II-11-1.

11. Cermak, J.E., "Laboratory Simulation of the Atmospheric Boundary Layer," AIAA J., Vol. 9, 1971, pp. 1746-1754.

12. Sundaram, T.R., Ludwig, G.R., and Skinner, G.T., "Modeling of the Turbulence Structure of the Atmospheric Surface Layer," AIAA J., Vol. 10, 1972, pp. 743-750.

13. Armitt, J., and Counihan, J., "The Simulation of the Atmospheric Boundary Layer in a Wind Tunnel," Atmospheric Environment, Vol. 2, 1968, pp. 49-71.

14. Blackadar, A.K., and Tennekes, H., "Asymptotic Similarity in Neutral Barotropic Planetary Boundary Layers," J. Atmos. Sciences, Vol. 25, 1968, pp. 1015-1020.

15. Plate, E.J., Aerodynamic Characteristics of Atmospheric Boundary Layers, Natl. Tech. Inform. Service TID-25465, 1971.

16. Rider, N.E., "The Effect of a Hedge on the Flow of Air," Quarterly J. Royal Meteorological Soc., Vol. 78, 1952, pp. 97-101.

APPENDIX

The internal boundary layer concept has been applied to wake flow. Fig. A1 shows upper and lower knees in wake velocity profiles. These knees mark the edge of regions of influence; the upper knee marks the outer edge of the internal boundary layer and the lower knee the edge of the sublayer. Fig. A2 shows a correlation of these data; the layers grow according to $x^{1/2}$.

A jet type correlation is used for velocity profiles near the building, and it is seen from Fig. A3 that the data are correlated by a single curve. Here ξ is the usual jet parameter $\sigma\ z'/x$. A similar correlation of turbulence data was attempted in Fig. A4. For the latter correlation to be useful a way of predicting u'_{max} must be found.

The decay of the velocity deficit is shown in Fig.A5. Presently a model is being developed to explain the change in slope of the decay curve.

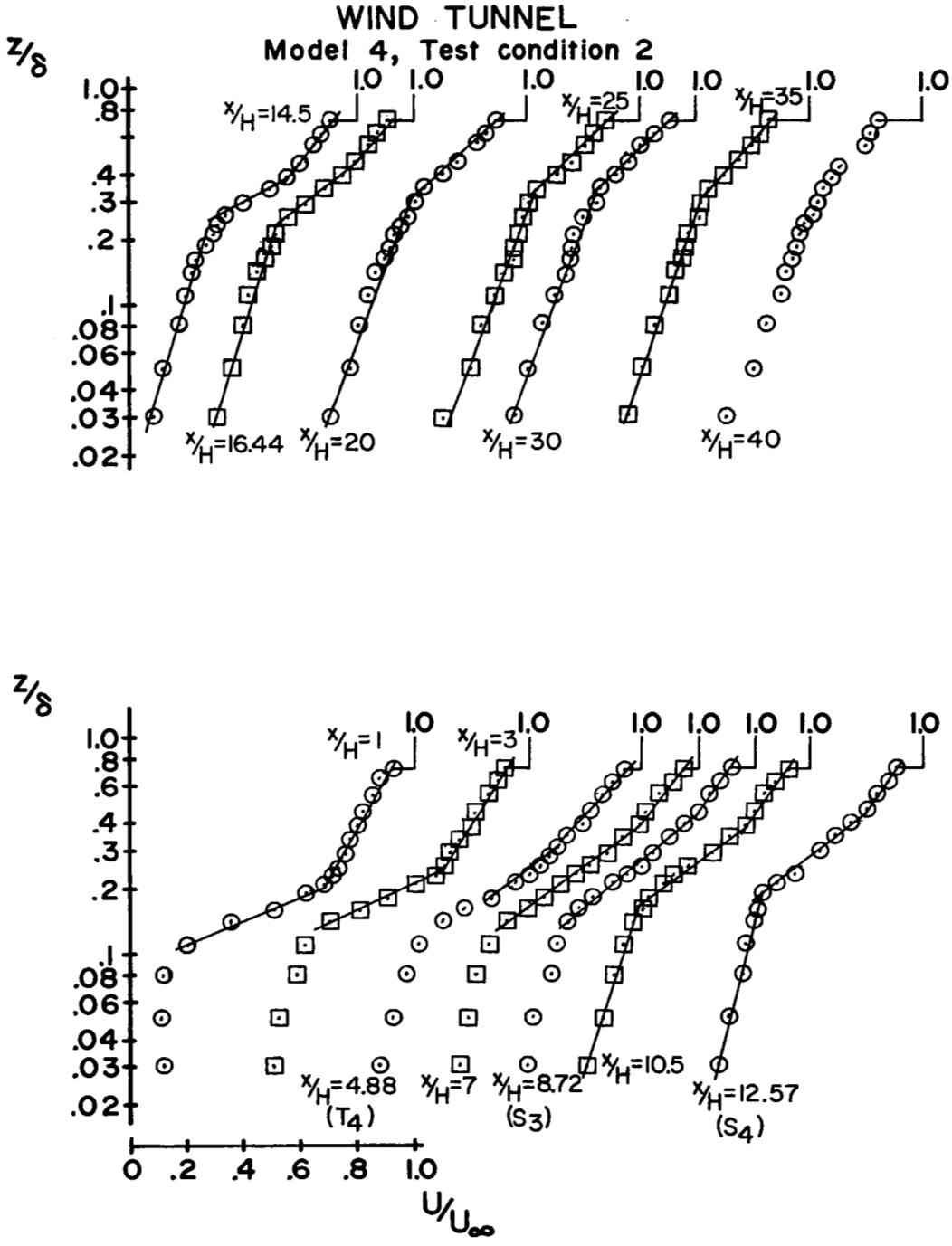

Fig. A1. Knee Points in Velocity Profiles

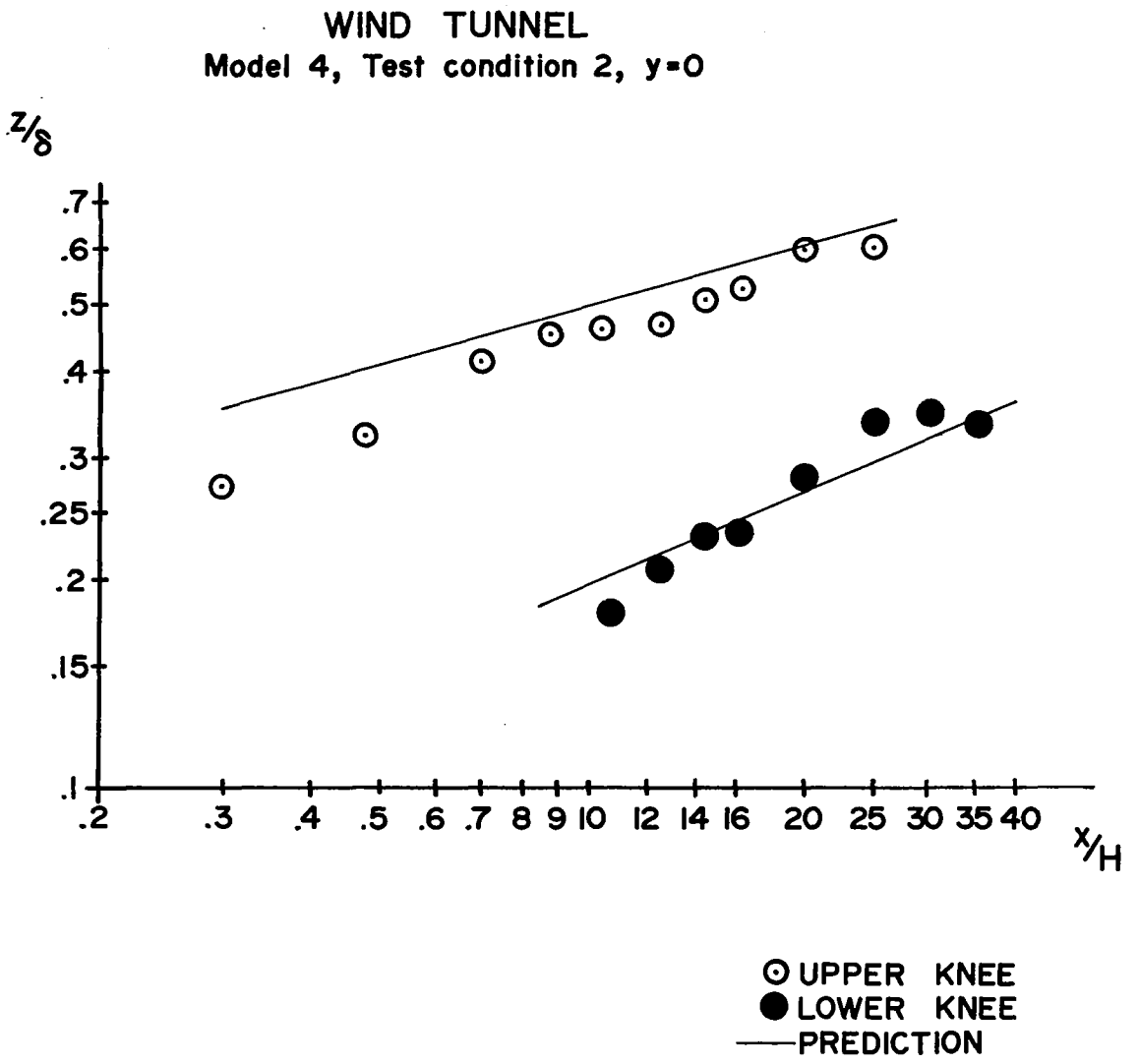

Fig. A2. Growth of Internal Boundary Layers

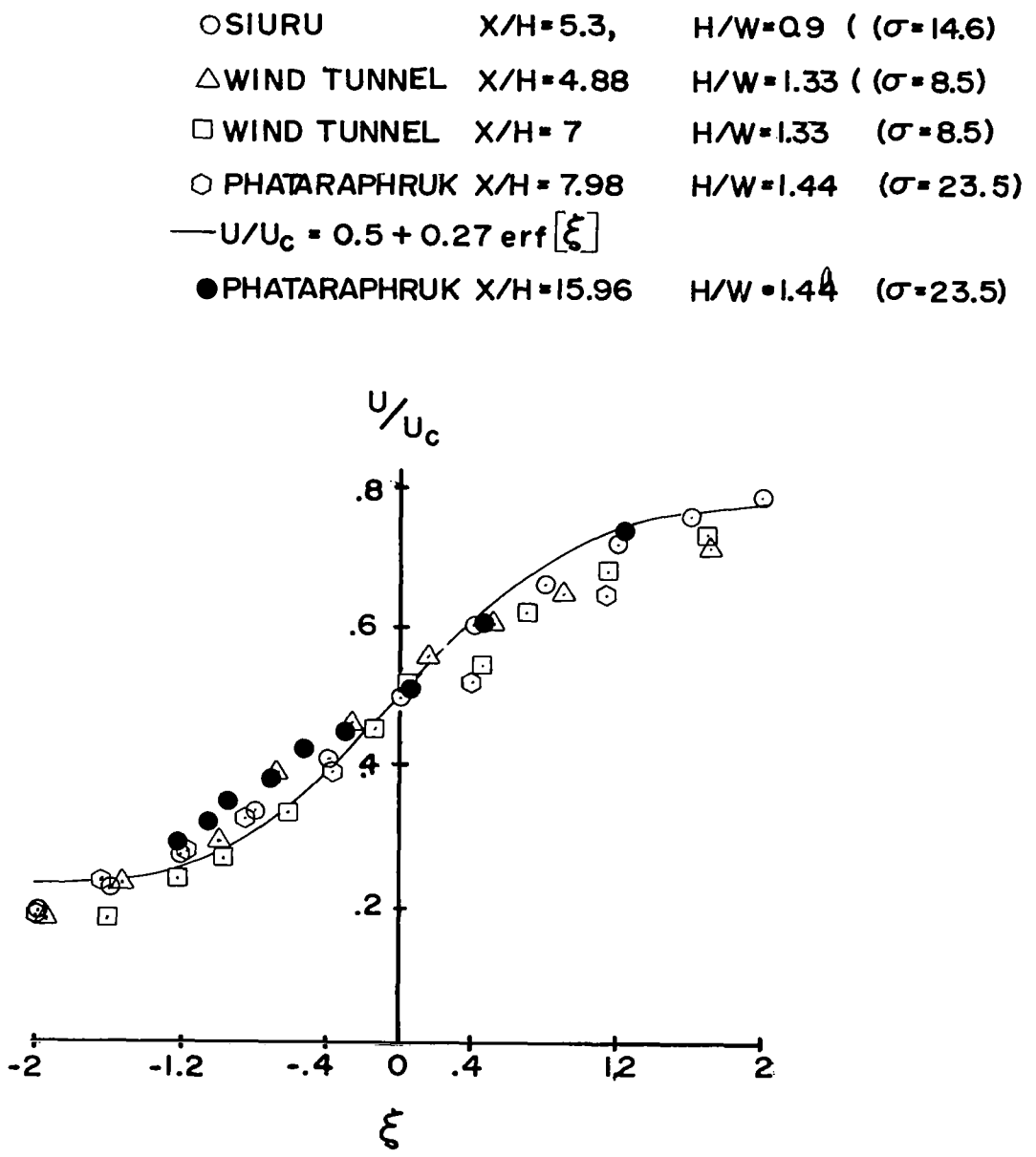

Fig. A3. Velocity Correlation in Near Wake

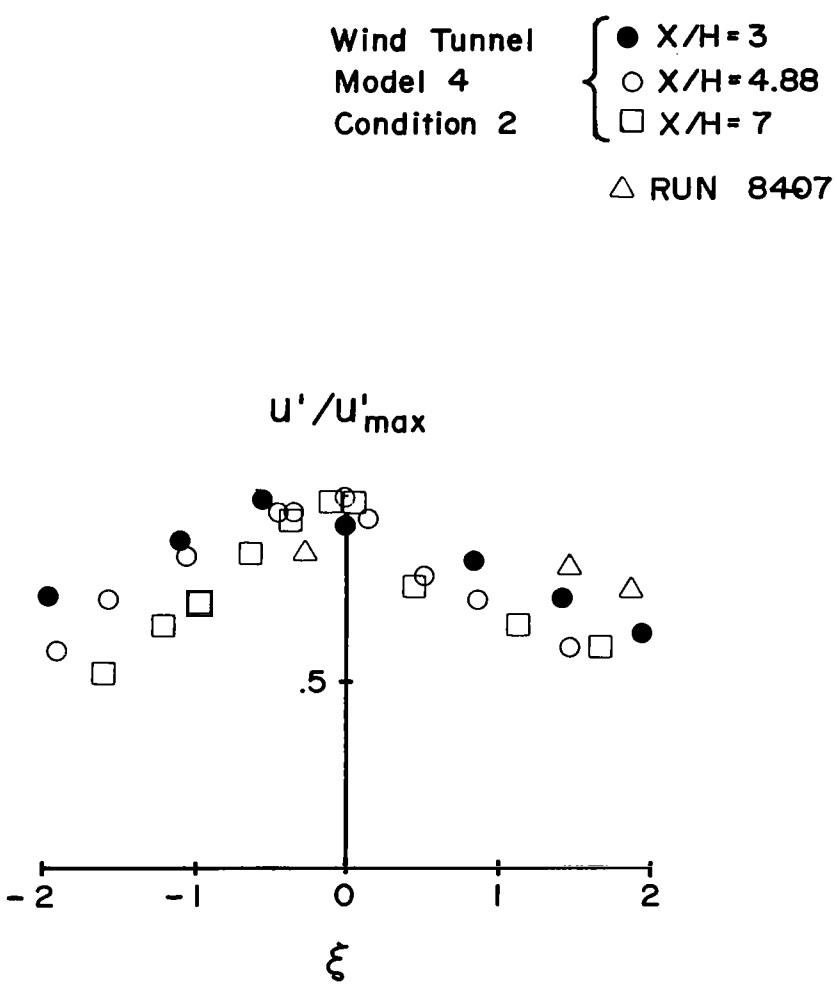

Fig. A4. Turbulence Correlation in Near Wake

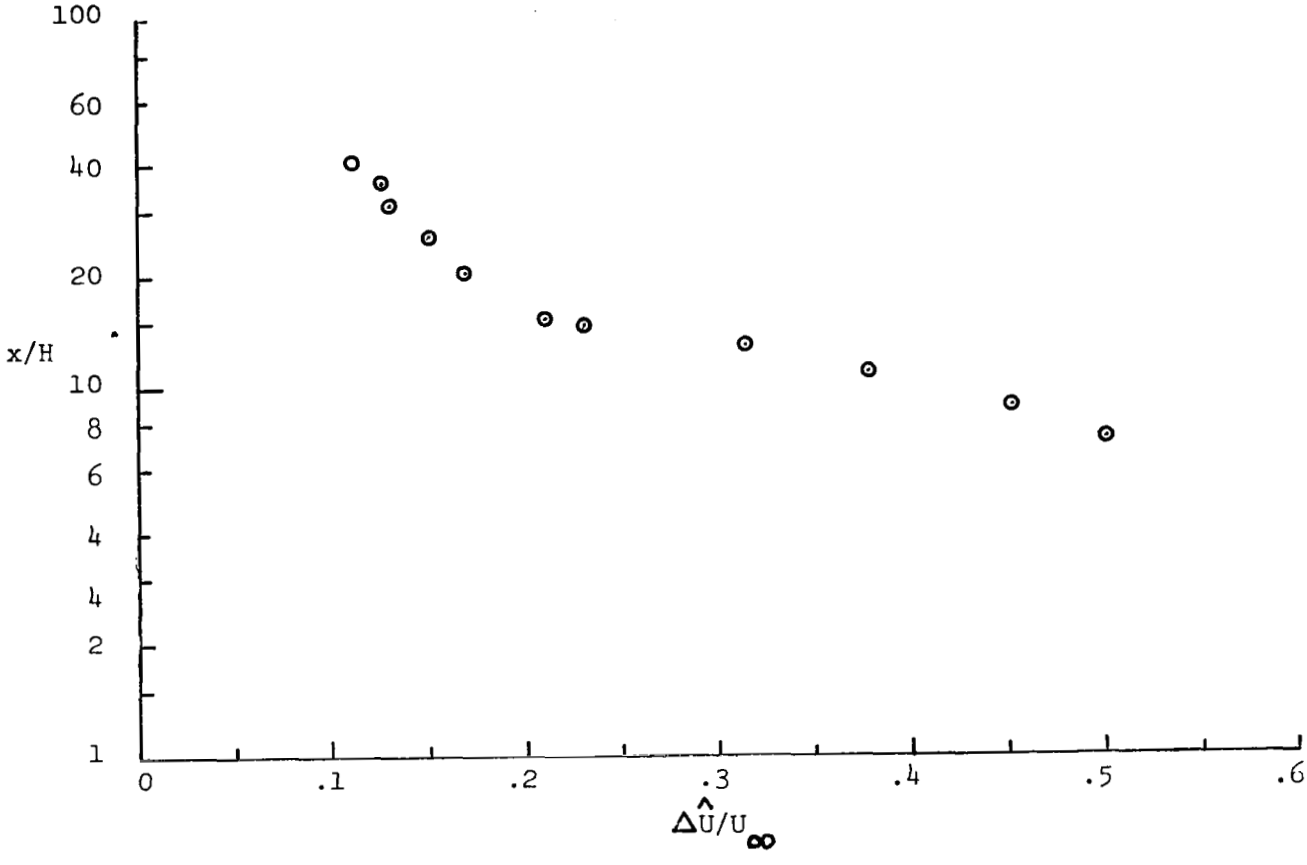

Fig. A5. Maximum Velocity Deficit in Wake

1. REPORT NO.	2. GOVERNMENT ACCESSION NO.	3. RECIPIENT'S CATALOG NO.
NASA CR-3008		

4. TITLE AND SUBTITLE	5. REPORT DATE
A Comparison of Wake Characteristics of Model and Prototype Buildings in Transverse Winds	May 1978
	6. PERFORMING ORGANIZATION CODE
7. AUTHOR(S)	8. PERFORMING ORGANIZATION REPORT #
Earl Logan, Jr., Prapoj Phataraphruk, and Jingfa Chang	ERC-R-78008
9. PERFORMING ORGANIZATION NAME AND ADDRESS	10. WORK UNIT NO.
	M-256
Engineering Research Center Arizona State University Tempe, Arizona 85281	11. CONTRACT OR GRANT NO. NAS 8-32357
	13. TYPE OF REPORT & PERIOD COVERED
12. SPONSORING AGENCY NAME AND ADDRESS	Contractor
National Aeronautics and Space Administration Washington, D. C. 20546	14. SPONSORING AGENCY CODE

15. SUPPLEMENTARY NOTES

Prepared under the technical monitorship of the Atmospheric Sciences Division, Space Sciences Laboratory, Marshall Space Flight Center

16. ABSTRACT

Previously measured mean velocity and turbulence intensity profiles in the wake of a 26.8-m long building 3.2 m high and transverse to the wind direction in an atmospheric boundary layer several hundred meters thick are compared with profiles at corresponding stations downstream of a 1/50-scale model on the floor of a large meteorological wind tunnel in a boundary layer 0.61 m in thickness. The purpose of the work is to determine the validity of using model wake data to predict full-scale data. Preliminary results are presented which indicate that disparities can result from differences in relative depth of logarithmic layers, surface roughness, and the proximity of upstream obstacles.

17. KEY WORDS	18. DISTRIBUTION STATEMENT
	Category 47

19. SECURITY CLASSIF. (of this report)	20. SECURITY CLASSIF. (of this page)	21. NO. OF PAGES	22. PRICE
Unclassified	Unclassified	55	$5.25

* For sale by the National Technical Information Service, Springfield, Virginia 22161

NASA-Langley, 1978